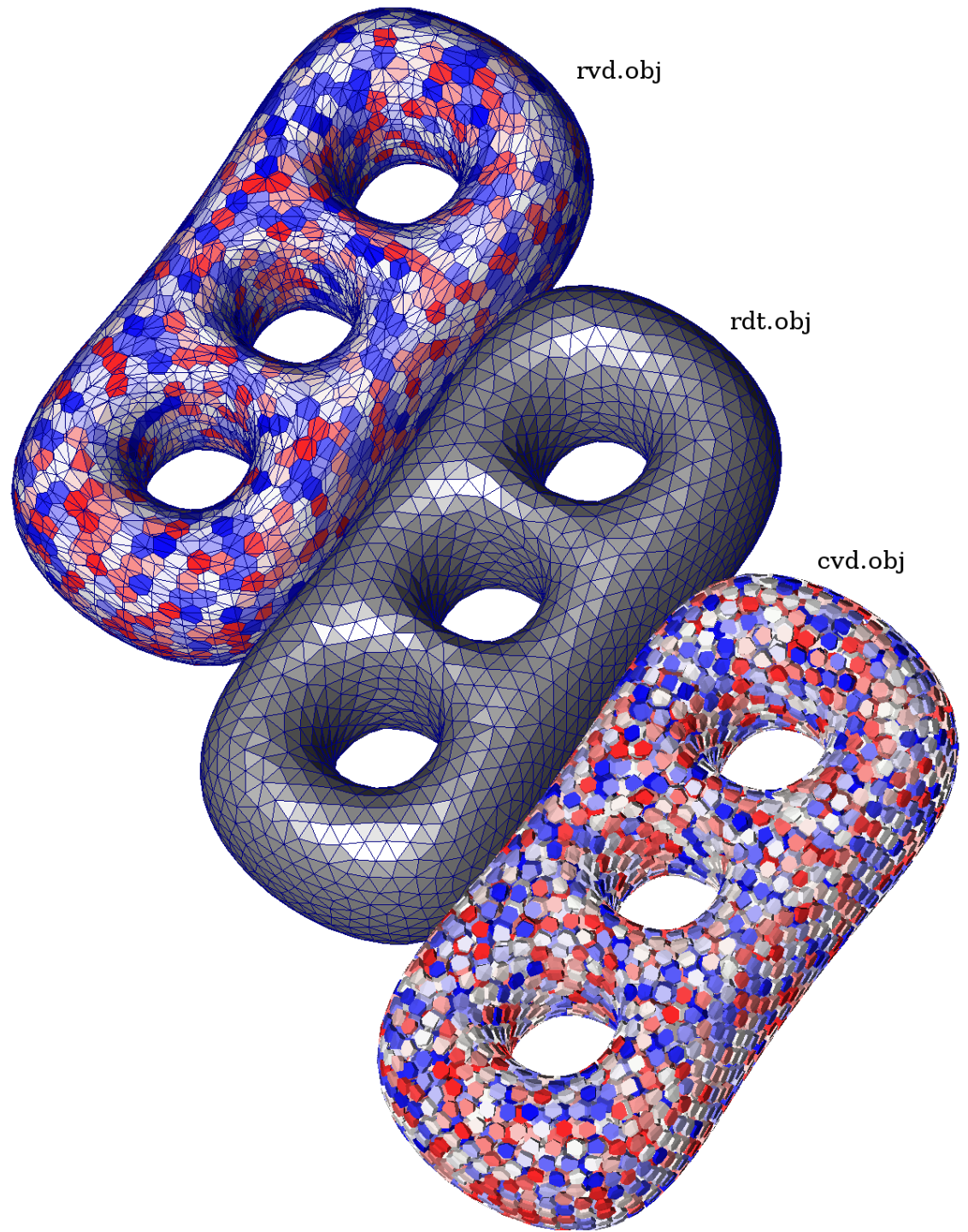
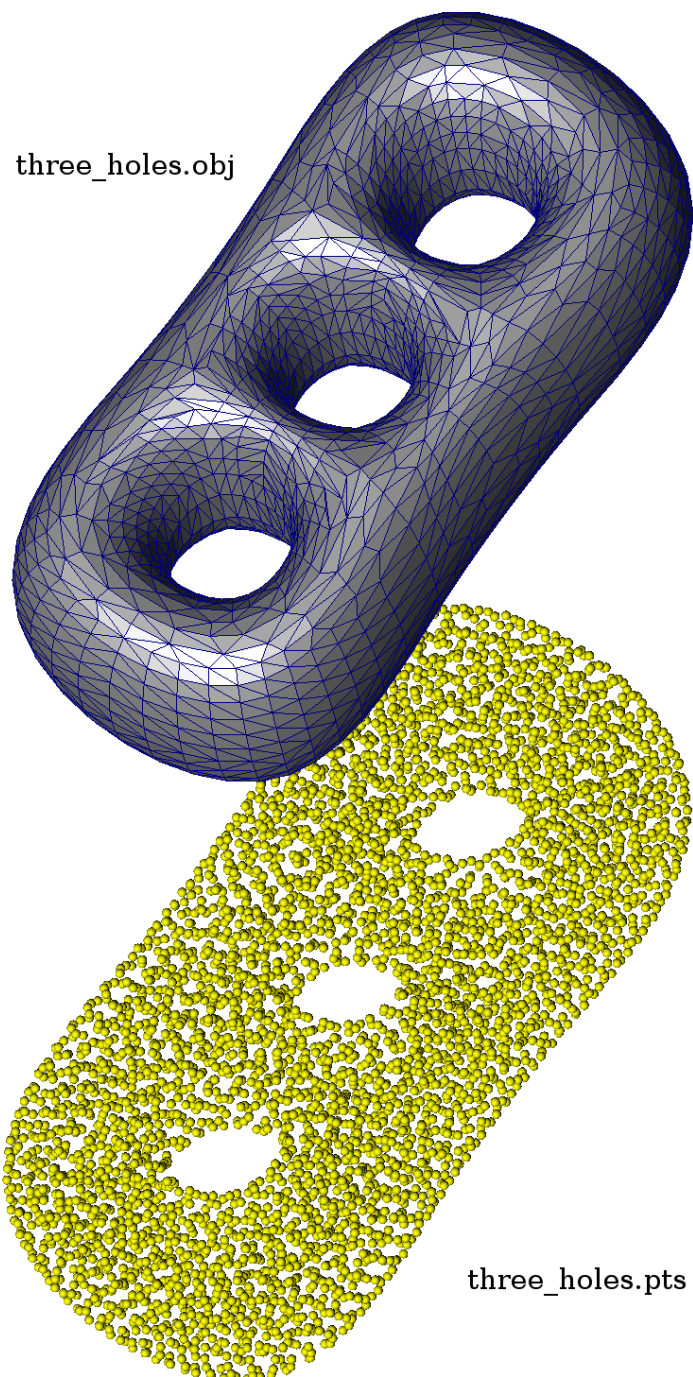
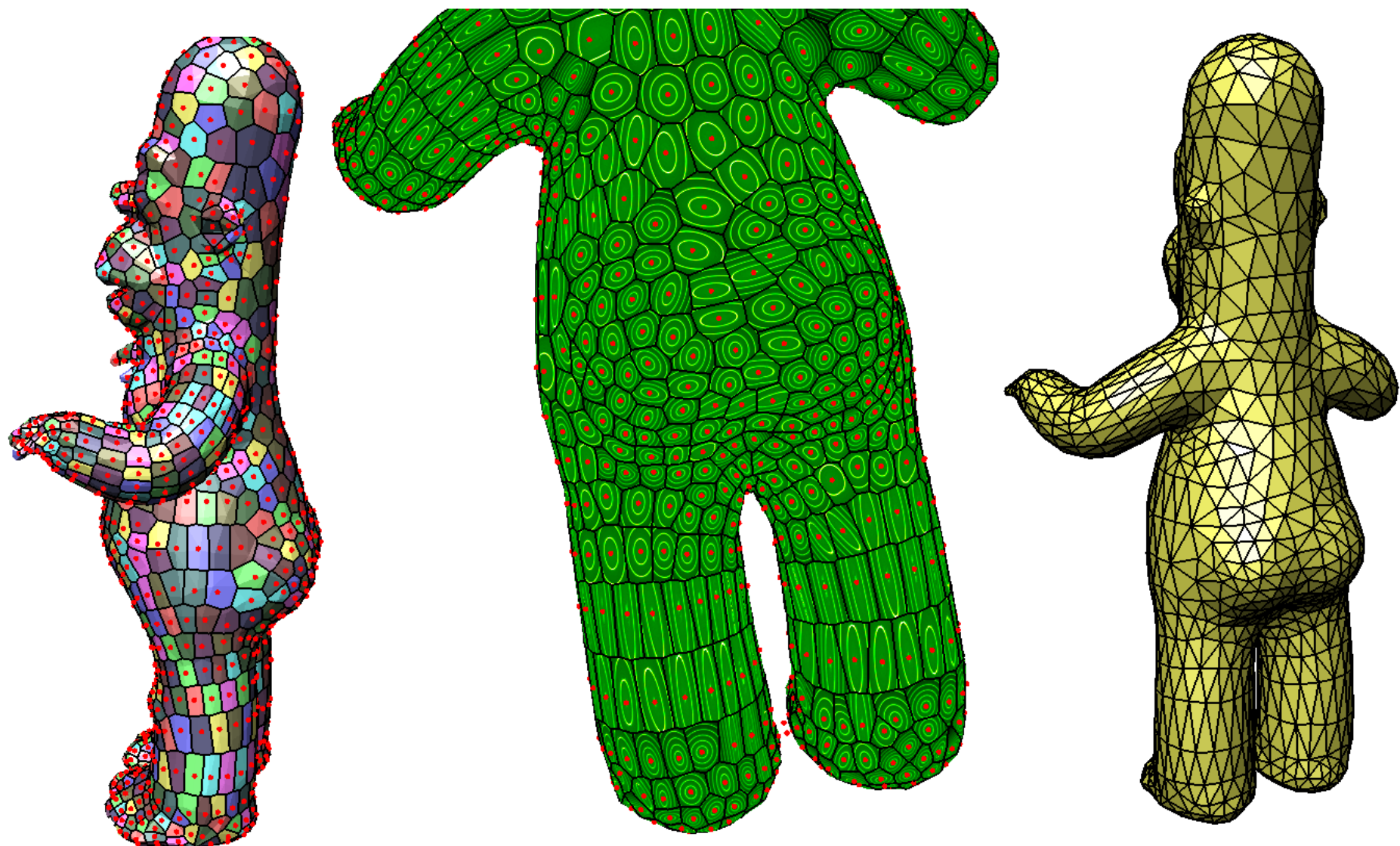


Supplemental material for paper 206

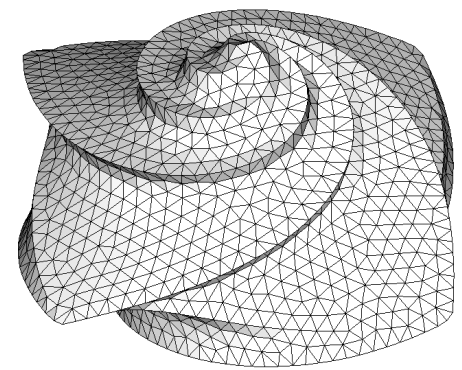
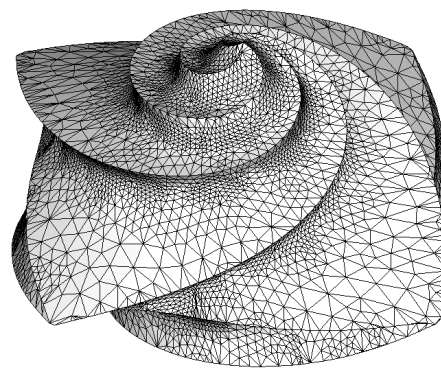
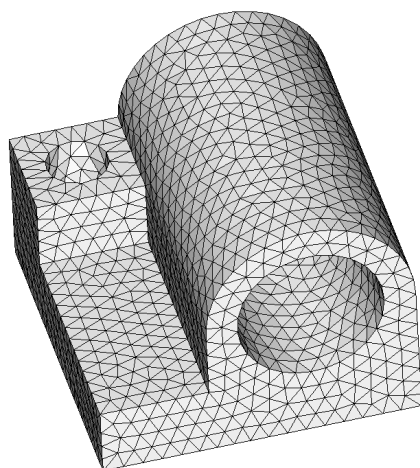
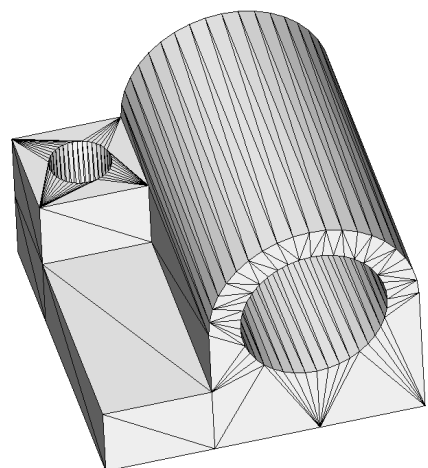
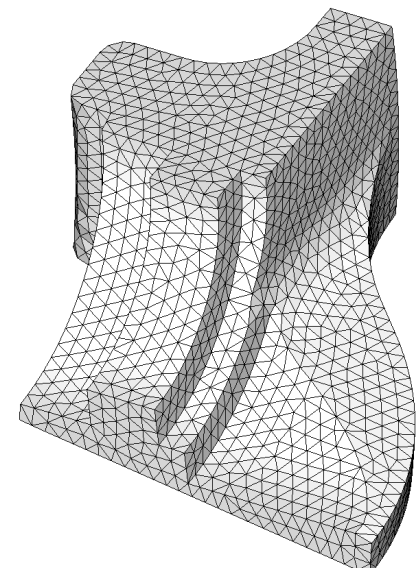
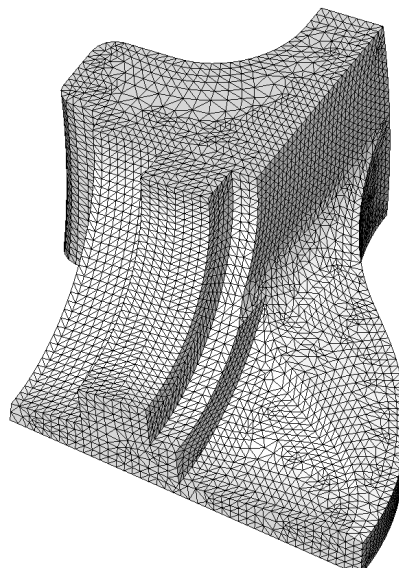
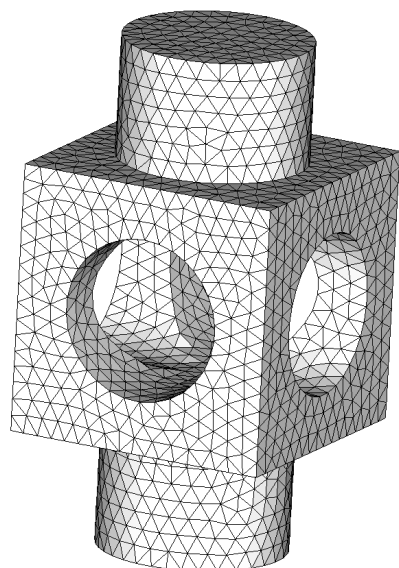
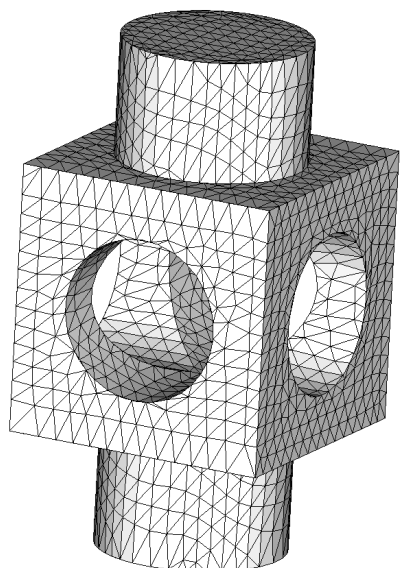
L_p Centroidal Voronoi Tessellation and its Applications



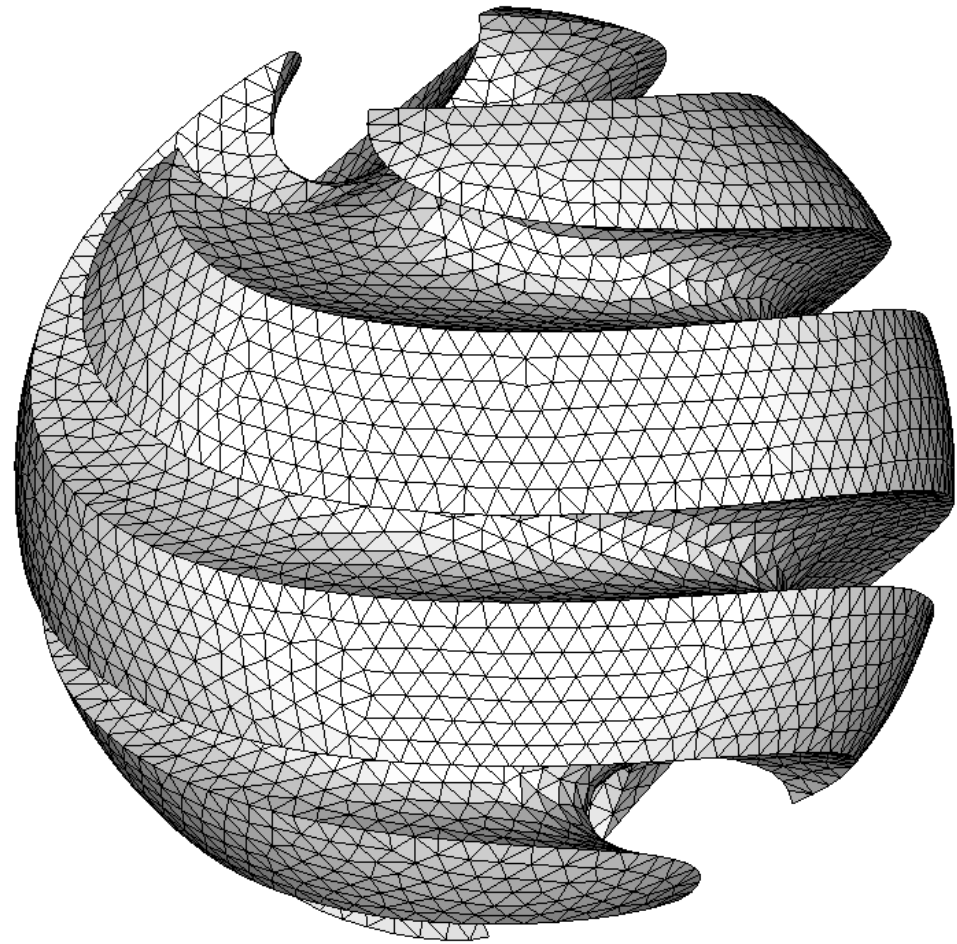
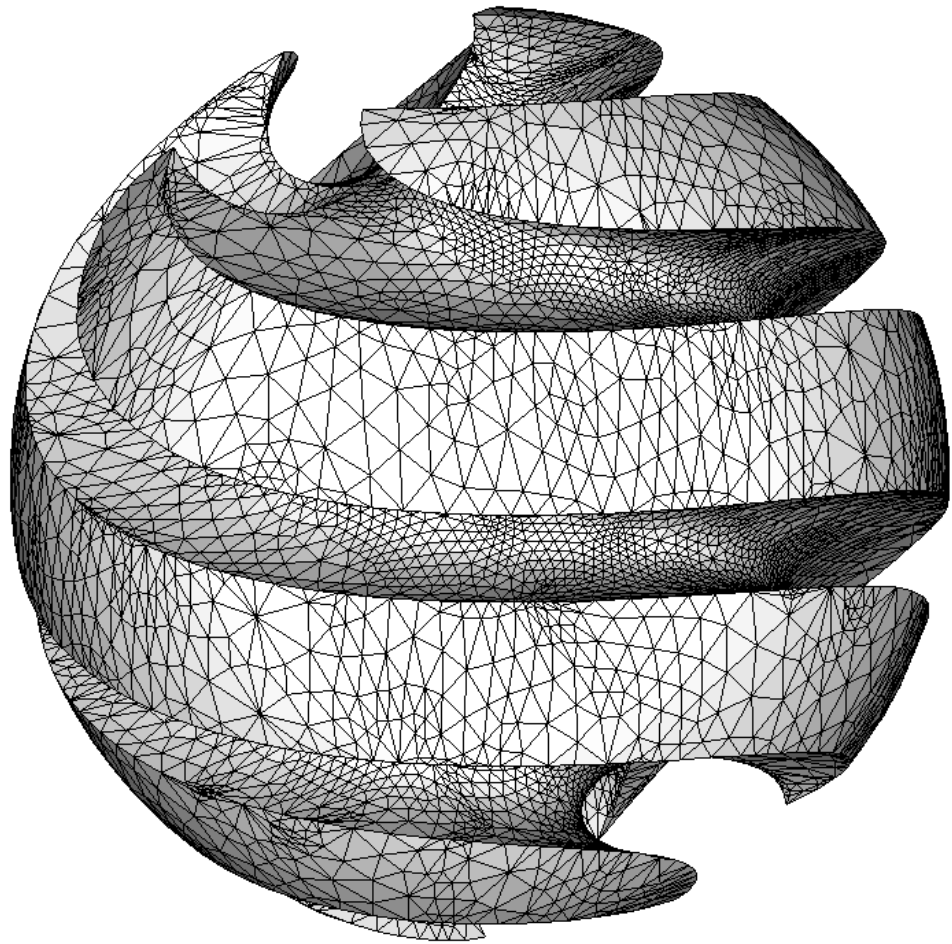
The C++ source code (also provided in the supplemental material) generates the restricted Voronoi diagram (rvd.obj), the restricted Delaunay triangulation (rdt.obj) and the clipped Voronoi diagram (cvd.obj) from a surface (three_holes.obj) and a point set (three_holes.pts).



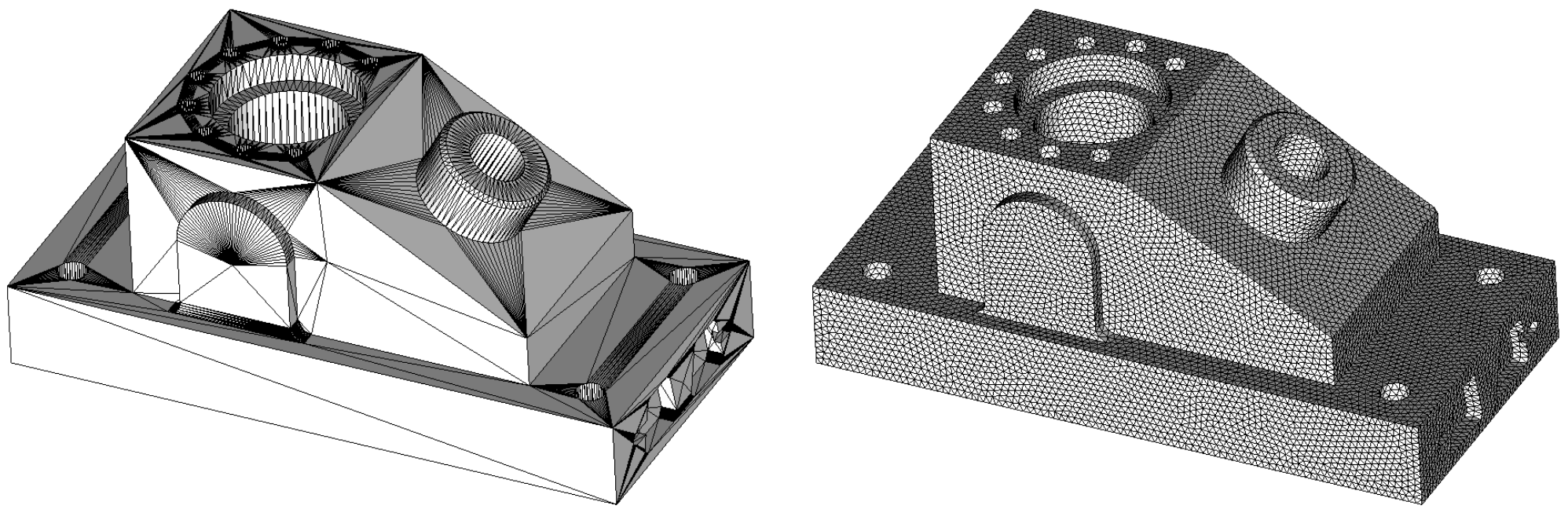
Anisotropic remeshing of 'homer'



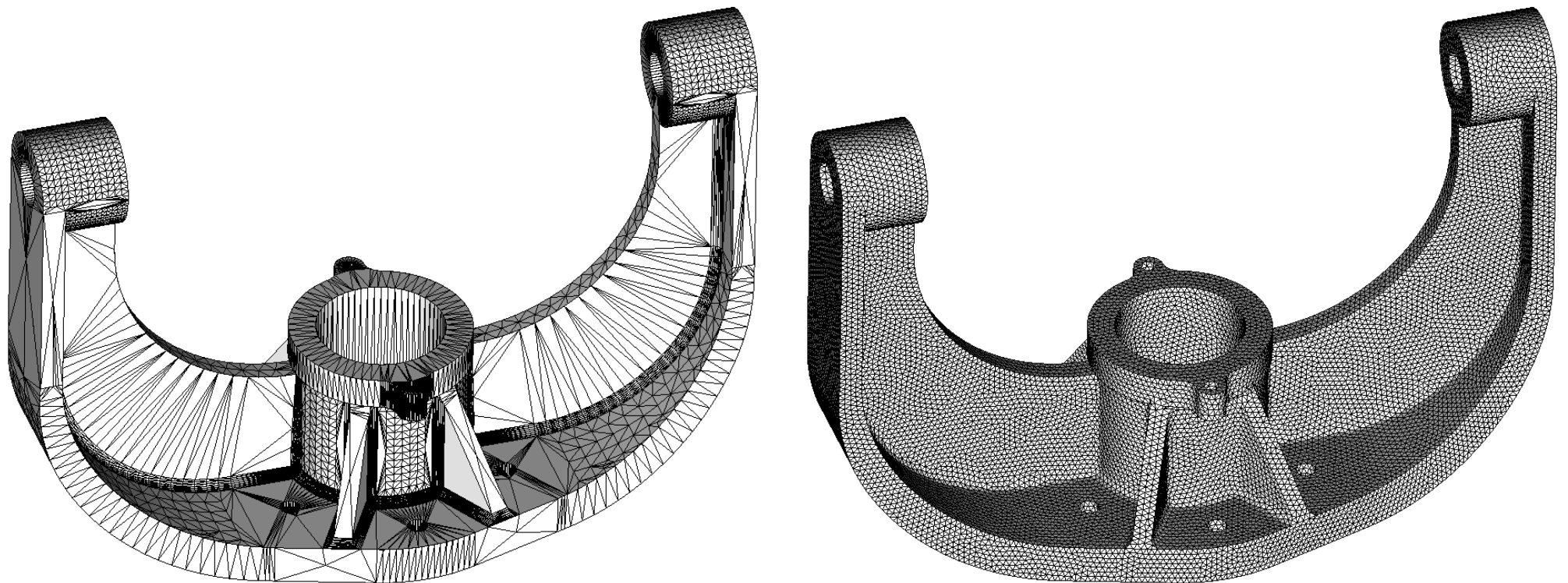
Remeshing simple examples with sharp features



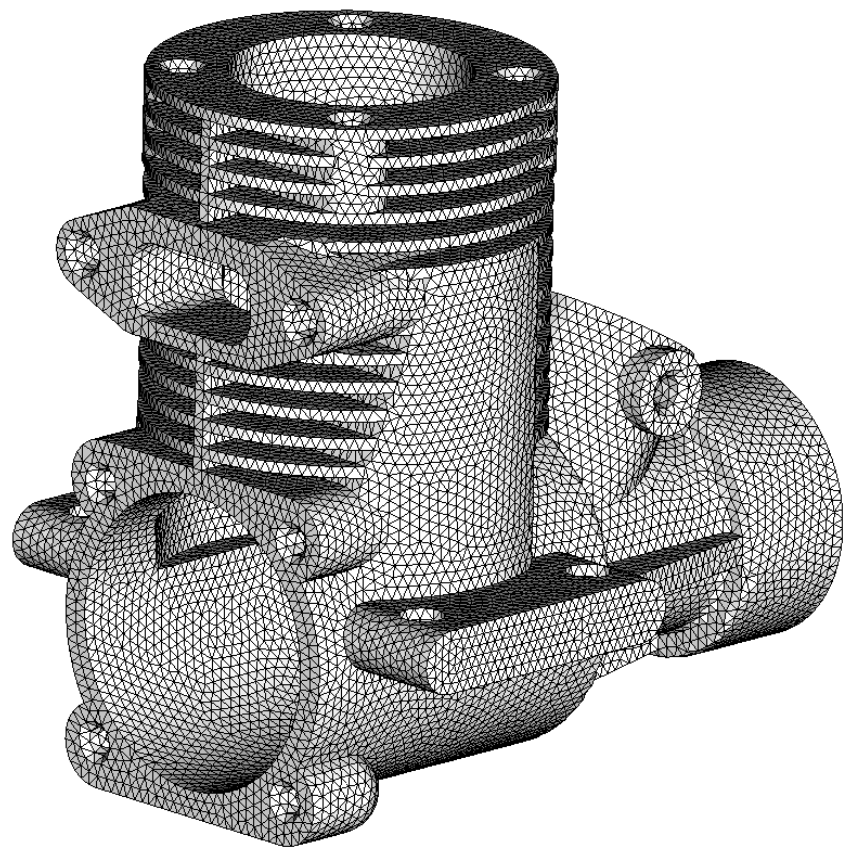
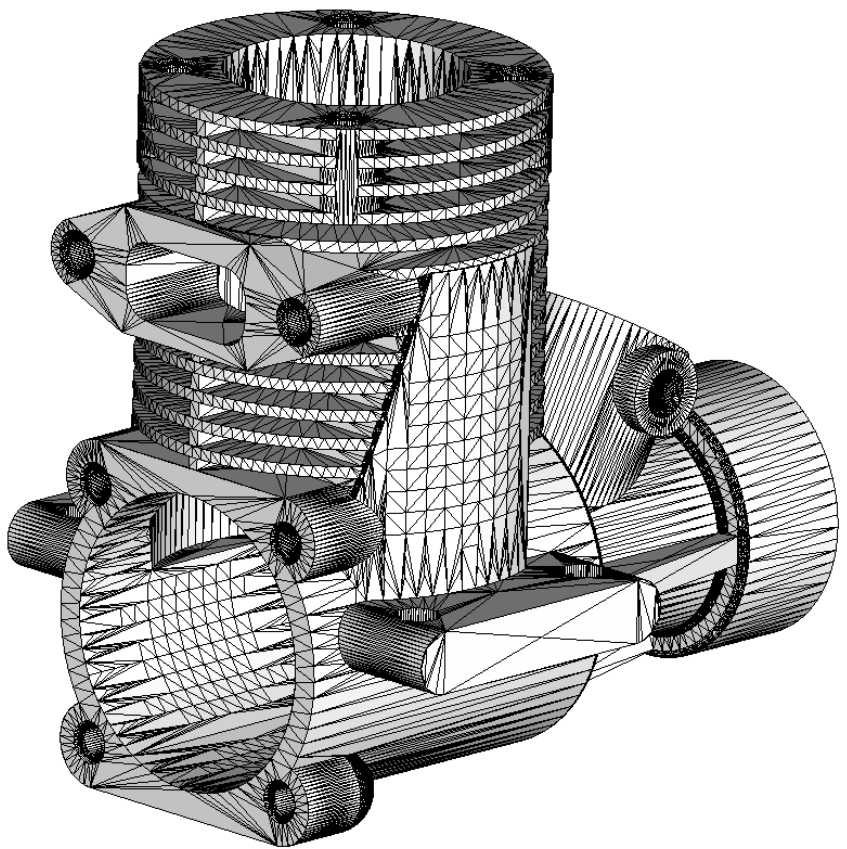
Remeshing a simple example with sharp features



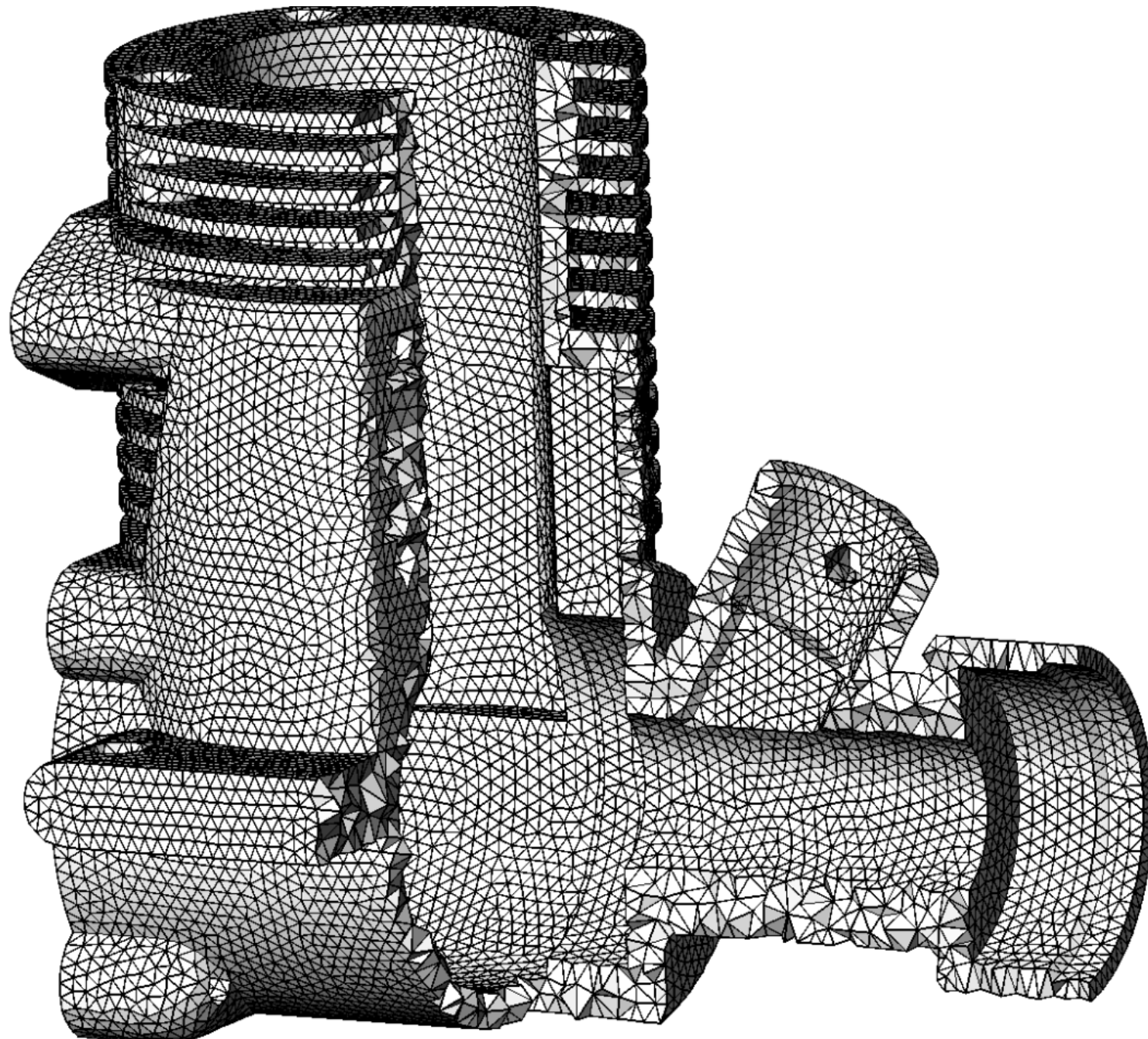
Remeshing a CAD model. Left: original data; Right: remesh



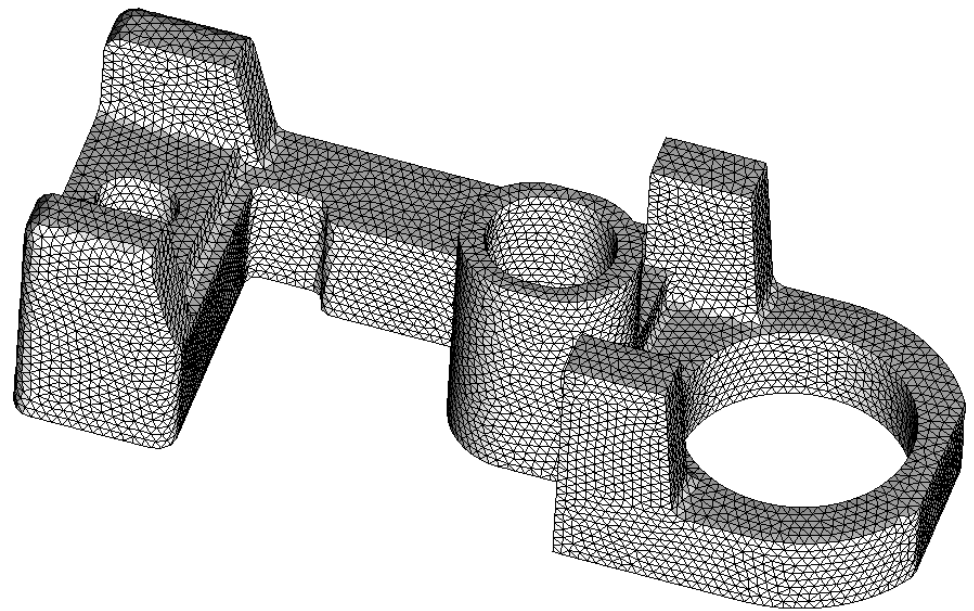
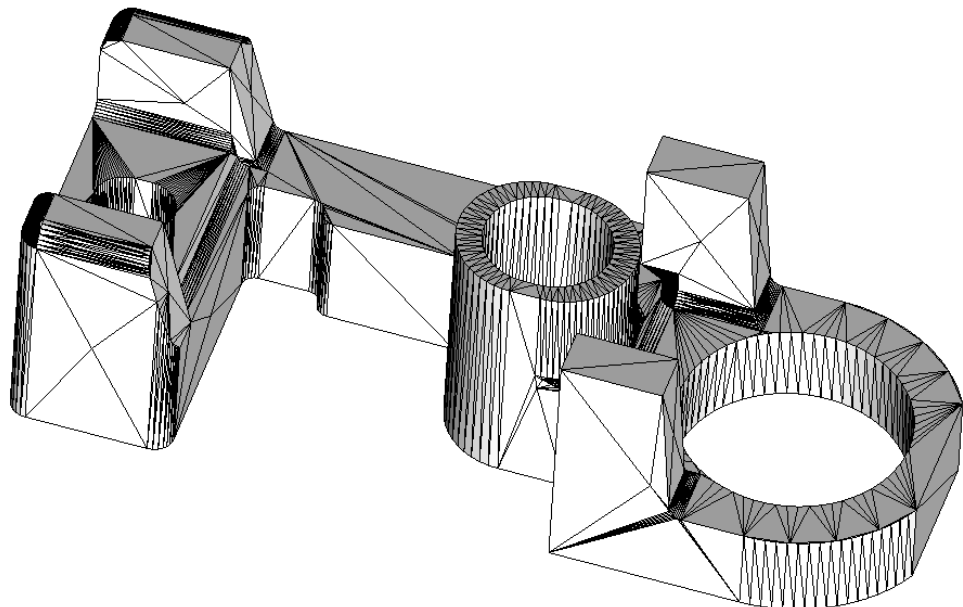
Remeshing a CAD model. Left: original data; Right: remesh



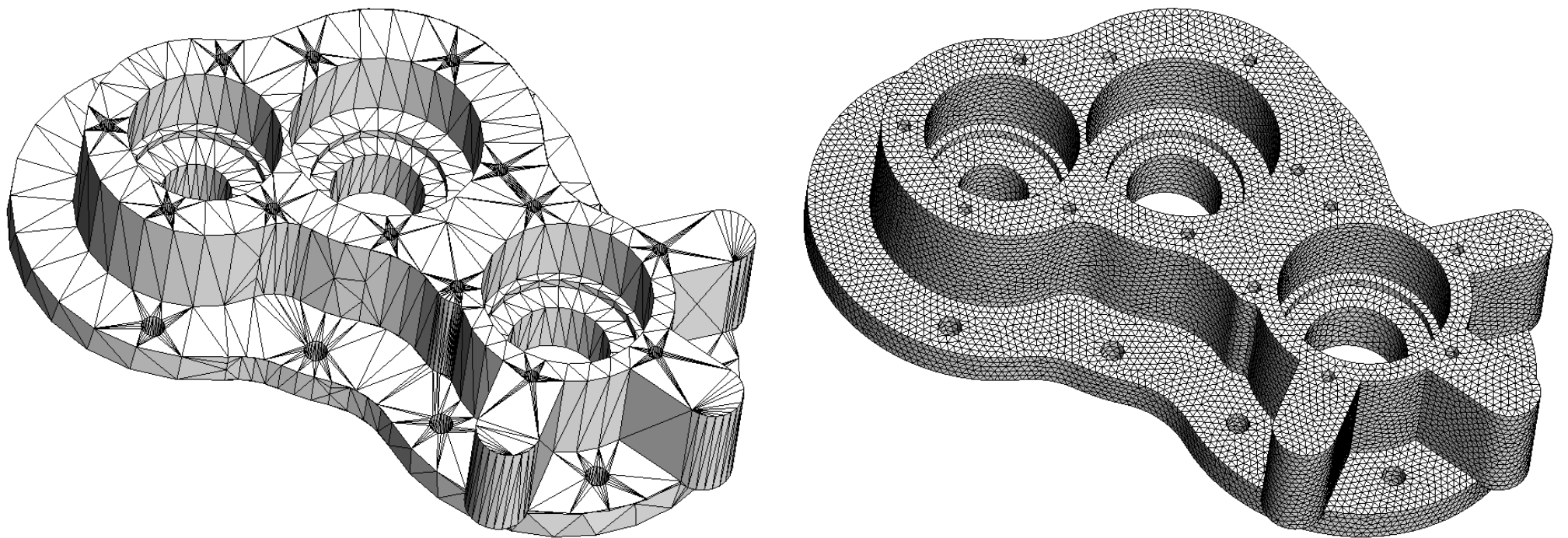
Remeshing a CAD model. Left: original data; Right: remesh



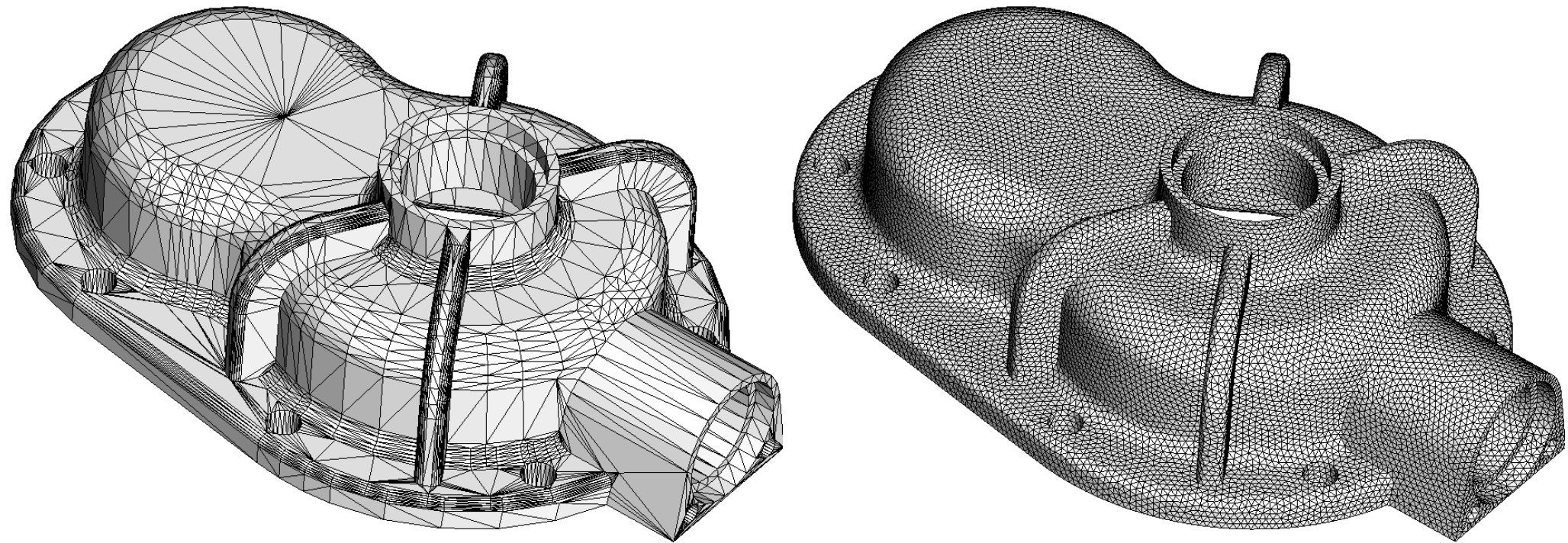
Tetrahedral mesh generated with tetgen from the remesh.



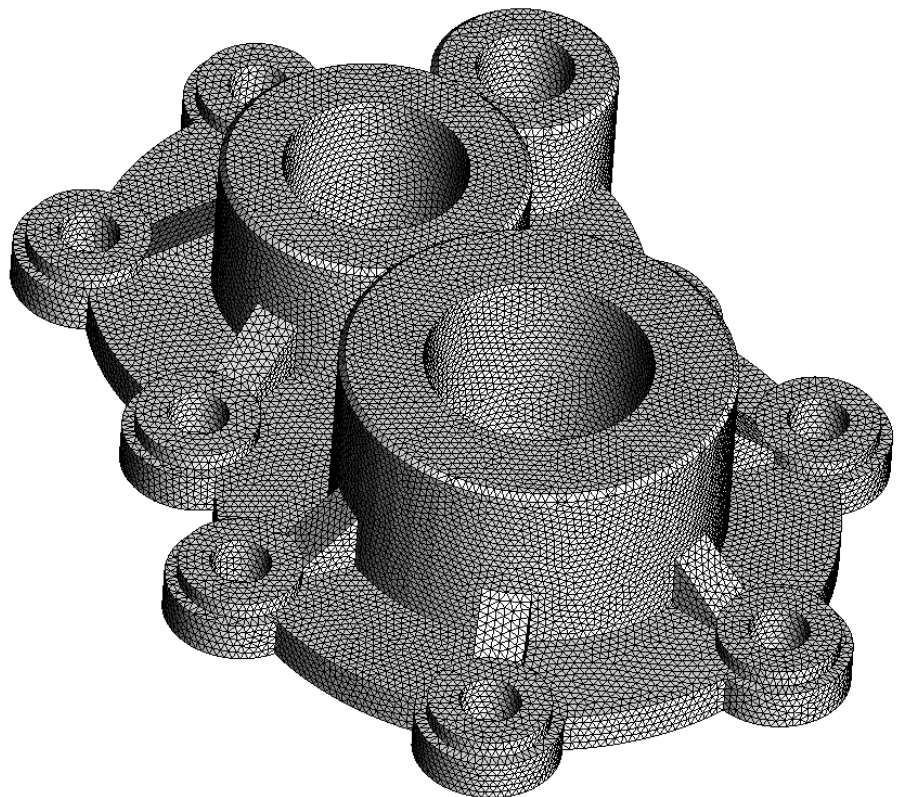
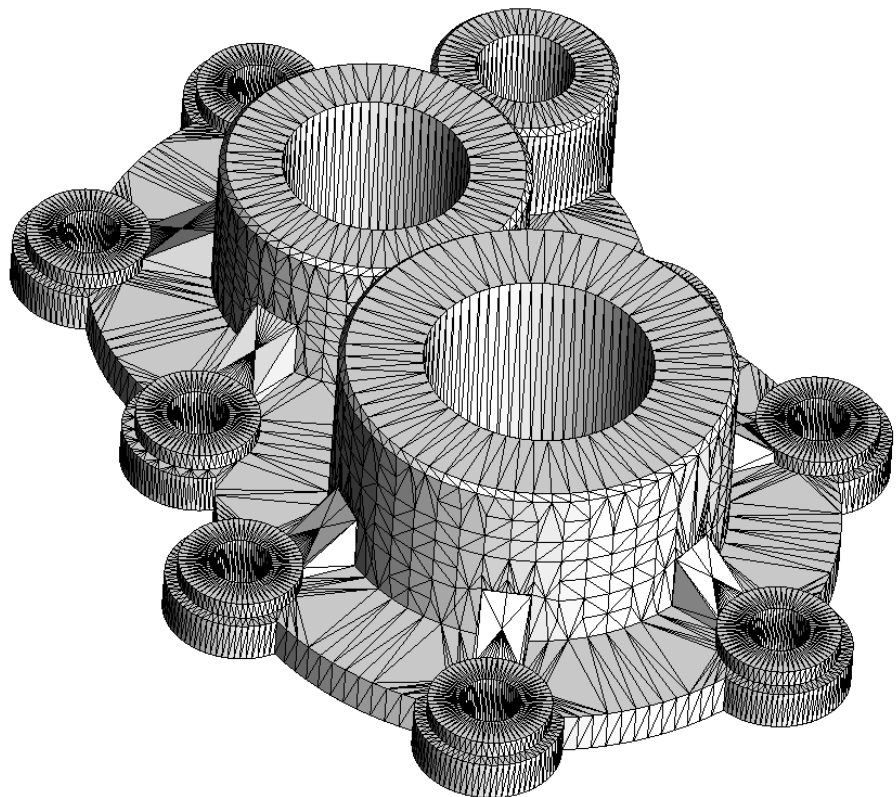
Remeshing a CAD model. Left: original data; Right: remesh



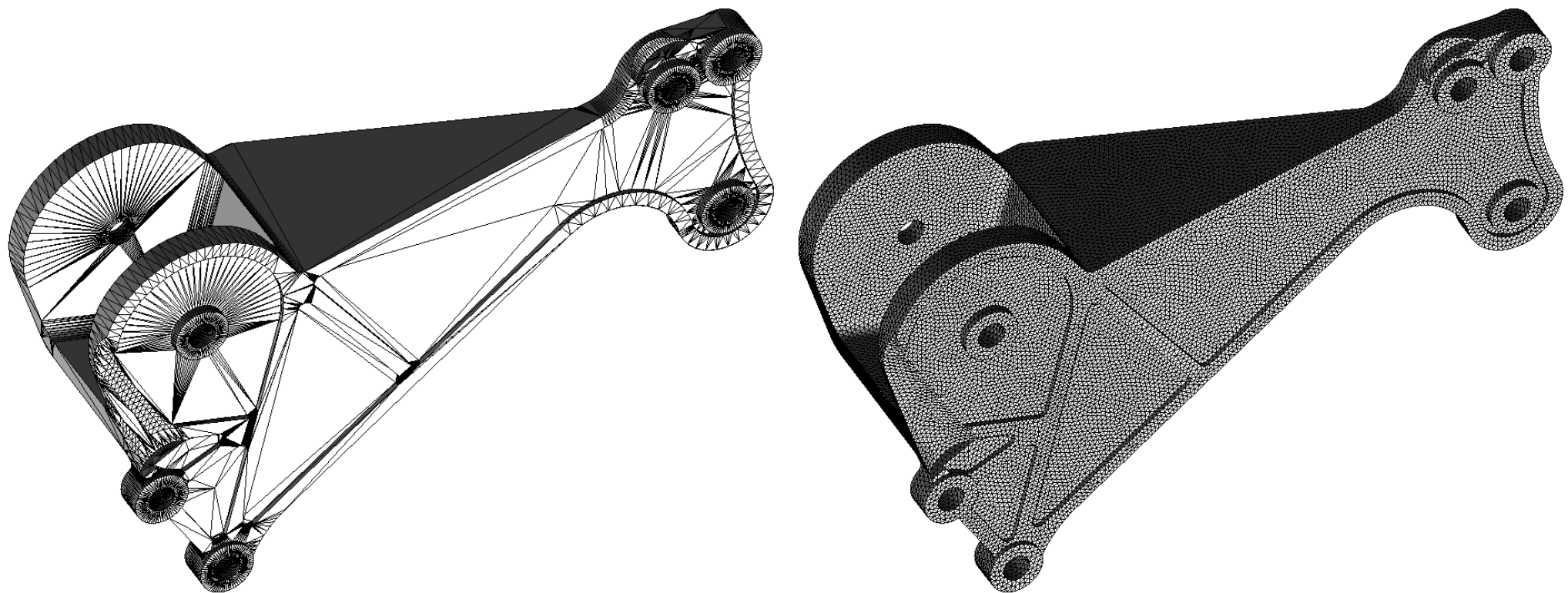
Remeshing a CAD model. Left: original data; Right: remesh



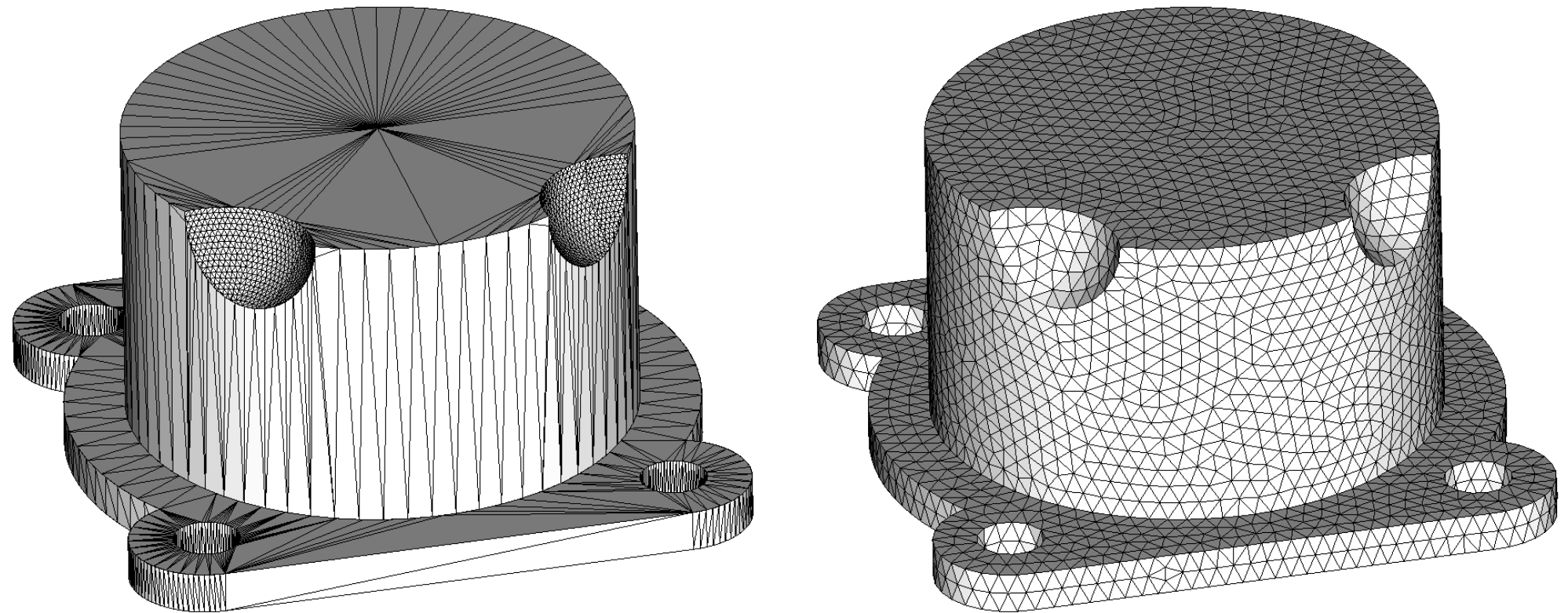
Remeshing a CAD model. Left: original data; Right: remesh



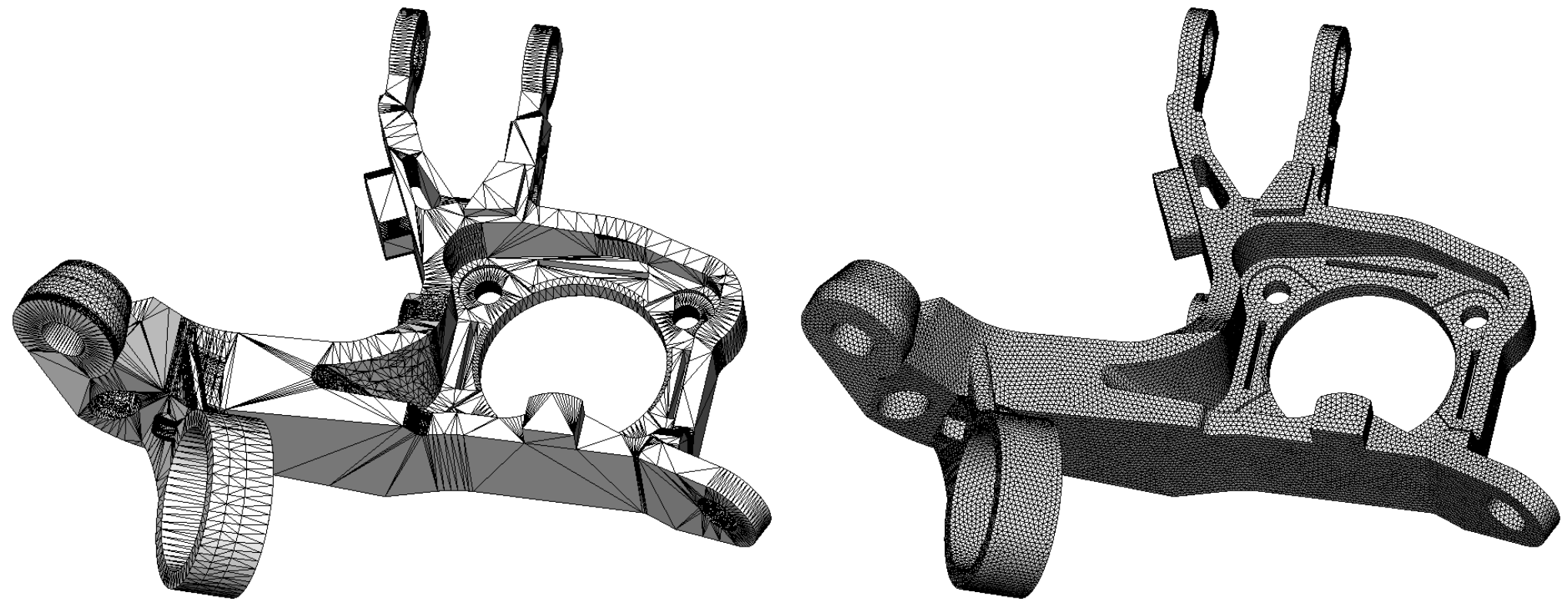
Remeshing a CAD model. Left: original data; Right: remesh



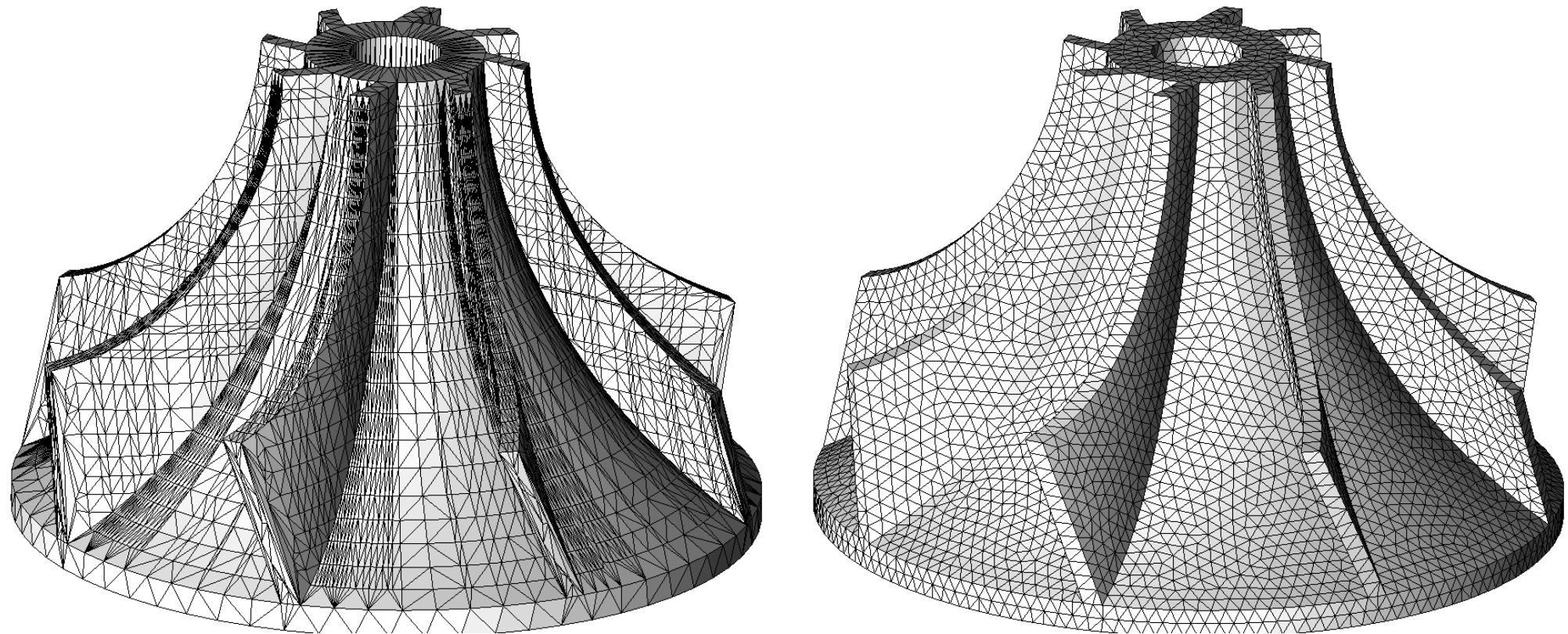
Remeshing a CAD model. Left: original data; Right: remesh



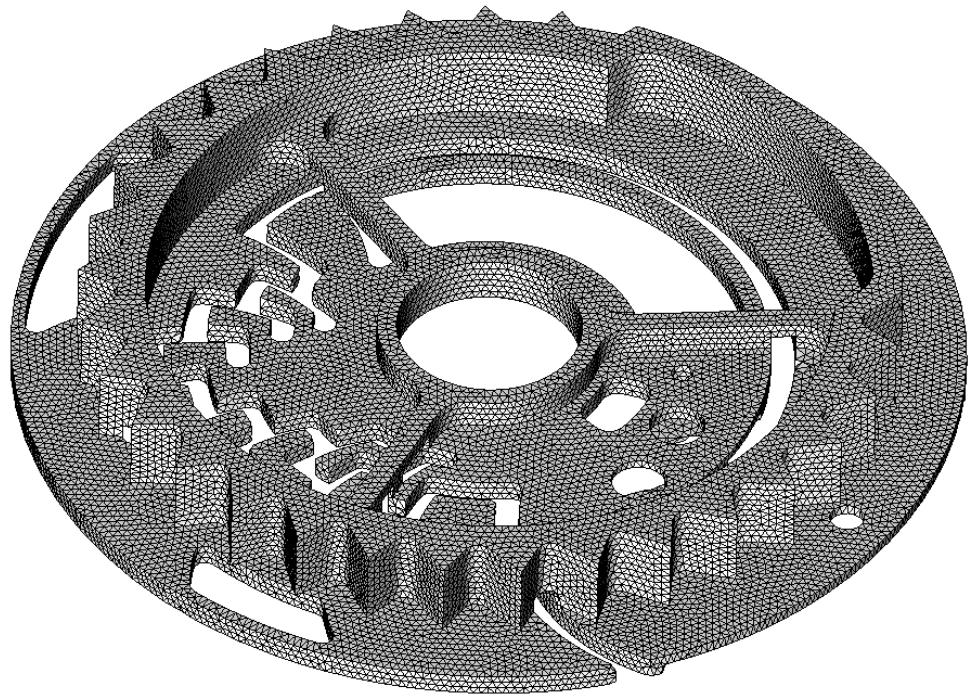
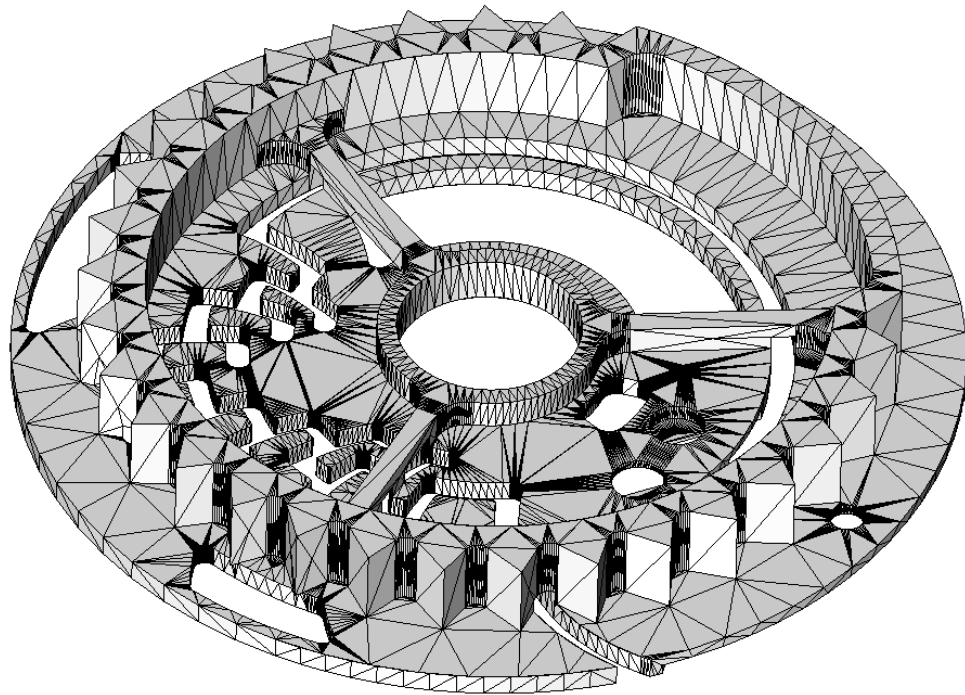
Remeshing a CAD model. Left: original data; Right: remesh



Remeshing a CAD model. Left: original data; Right: remesh



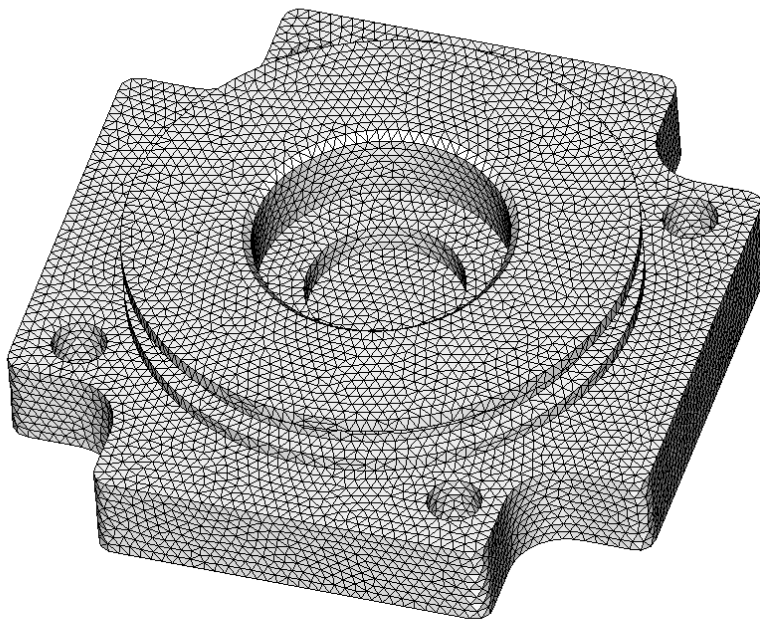
Remeshing a CAD model. Left: original data; Right: remesh



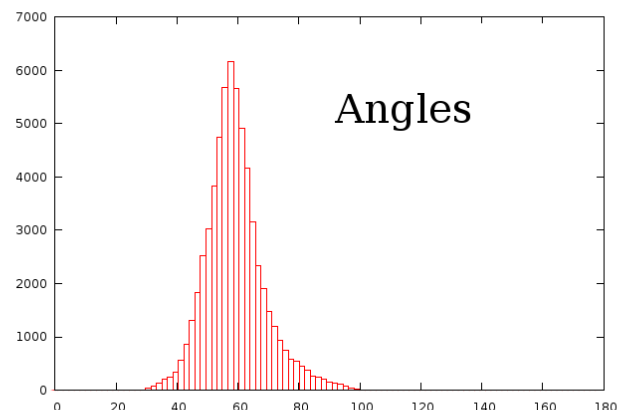
Remeshing a CAD model. Left: original data; Right: remesh



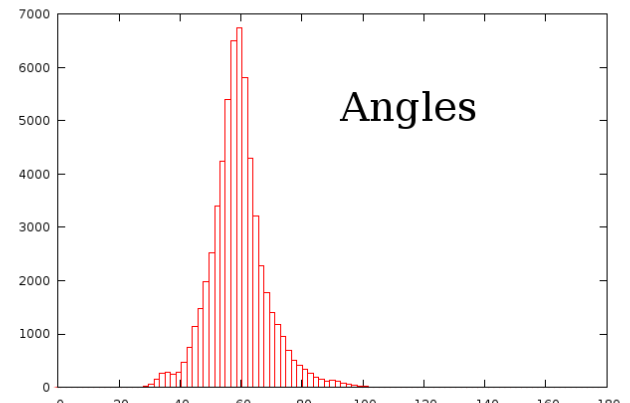
Remeshing a CAD model. Left: original data; Right: remesh



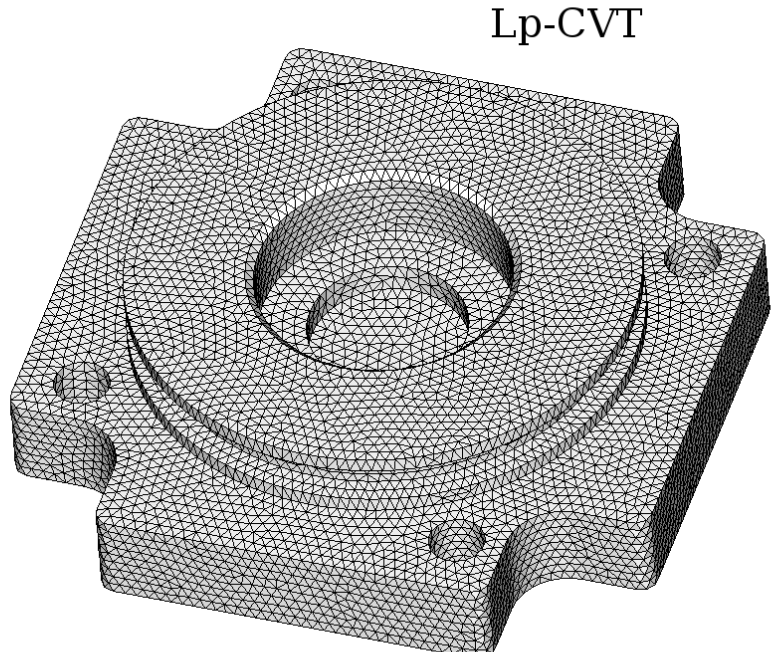
[Tournois et.al 2009]



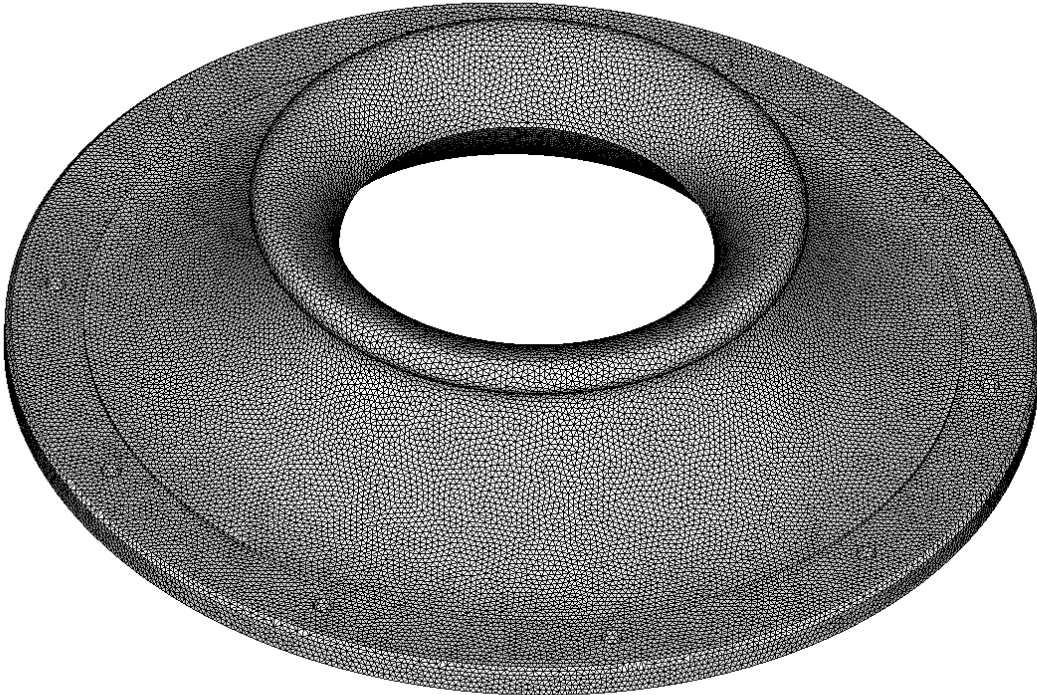
min: 27.45
max: 112.40



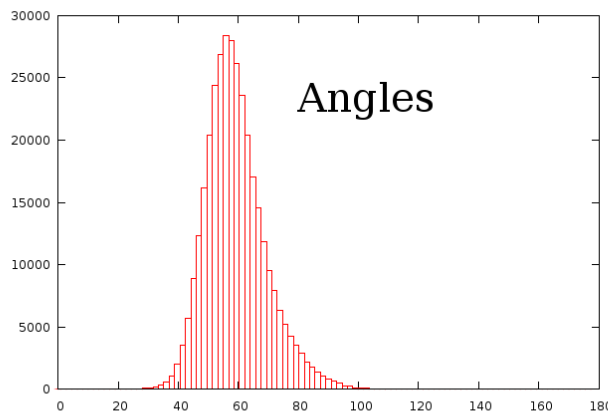
min: 28.34
max: 114.65



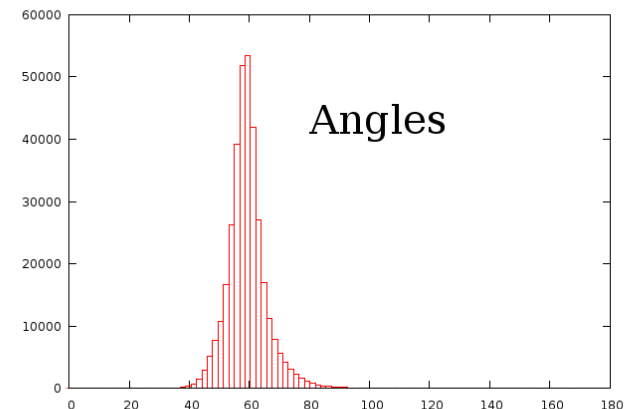
Comparison between surface L_p -CVT and the boundary of a tet mesh obtained by [Tournois et.al 2009] (same number of vertices). Data kindly provided by author.
A similar result is obtained. Note that unlike Tournois et.al's method, L_p -CVT does not require sharp features to be tagged.



[Tournois et.al 2009]

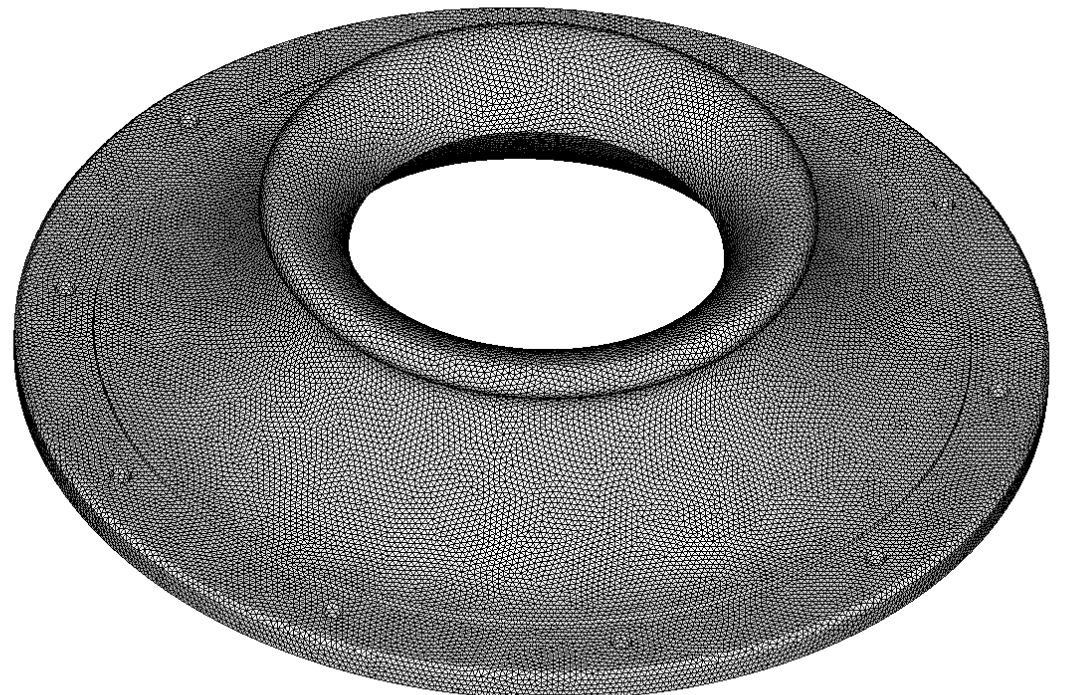


min: 11.45
max: 123.047



min: 33.10
max: 109.29

L_p-CVT



Comparison between surface L_p -CVT and the boundary of a tet mesh obtained by [Tournois et.al 2009] (same number of vertices). Data kindly provided by author. Better angles are obtained with L_p -CVT. We think this is because (1) [Tournois et.al 09] is a tet meshing algorithm, that is a more constrained problem than surface remeshing and (2) the closed form derivations in L_p -CVT and the more efficient Newton solver lead to a better optimum of the objective function.

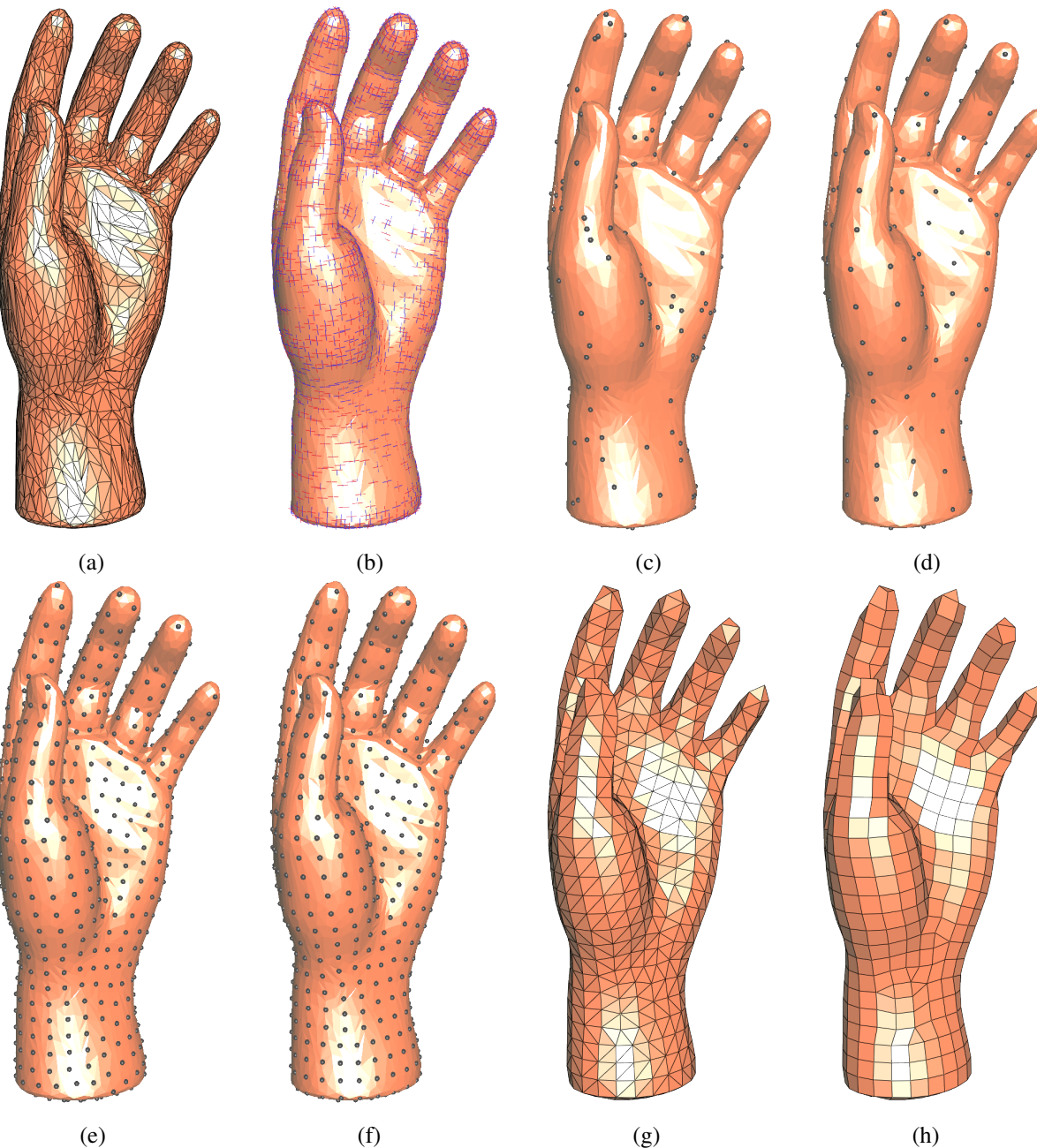


Figure 1: An illustration of L_p Quad-dominant meshing workflow. (a) an input mesh; (b) Anisotropy field computation; (c) 200 points are sampled on the input mesh randomly; (d) the point distribution after 30 iterations of L_p optimization; (e) Interleaved refinement. Insert a new point at the middle of each edge of the restricted Delaunay triangulation; (f) the point distribution after 30 iterations of L_p optimization; (g) the restricted Delaunay triangulation; (h) merge adjacent triangles into quadrilateral according to the quality of the quadrilateral.

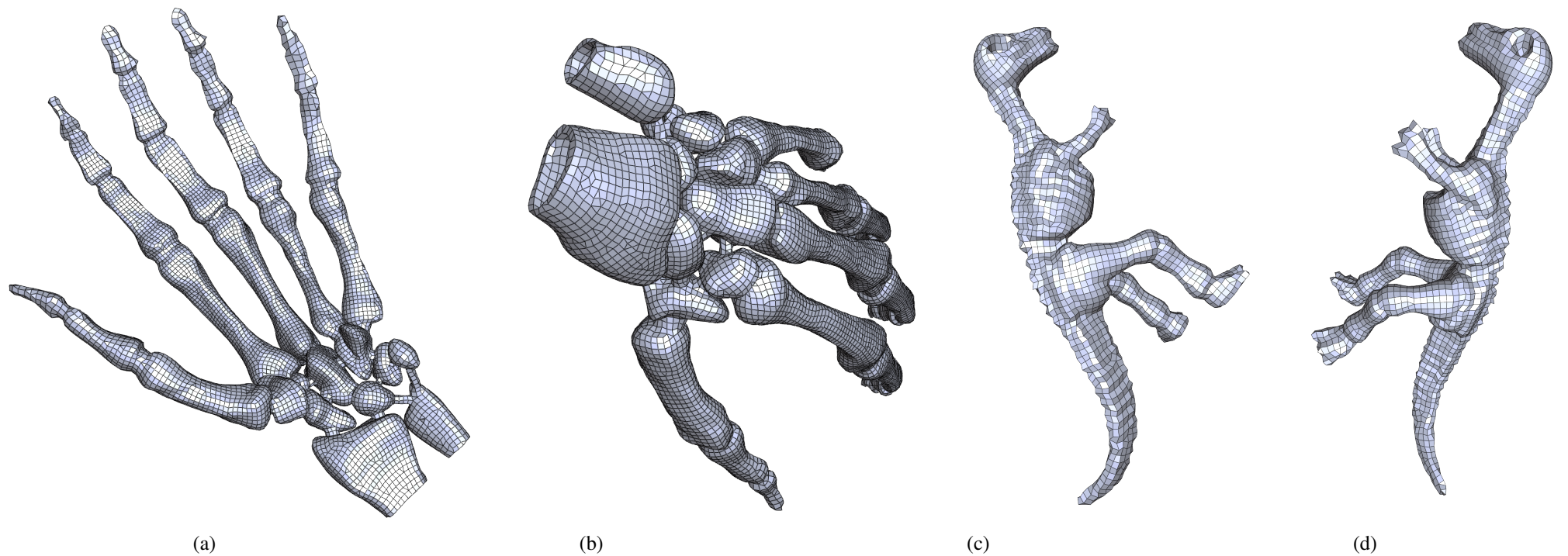


Figure 2: (a)&(b): Quad-dominant meshing of Hand model. (c)&(d): Quad-dominant meshing of Dinosaur model.

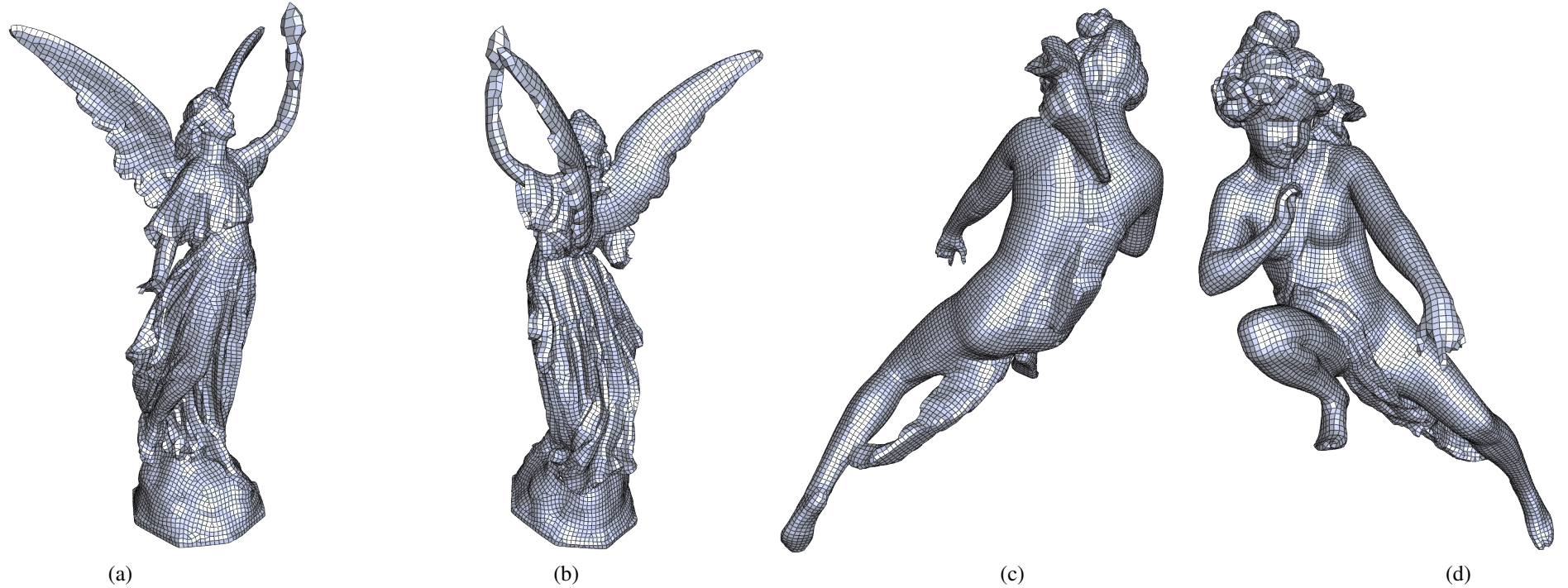


Figure 3: (a)&(b): Quad-dominant meshing of Lucy model; (c)&(d):Quad-dominant meshing of Angel model.

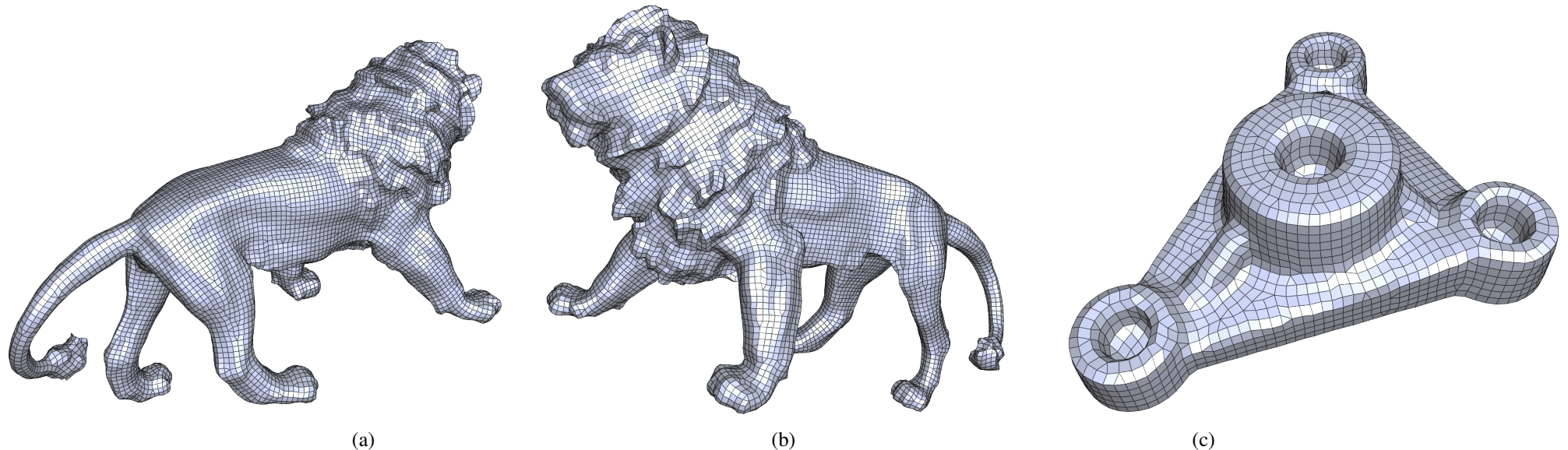


Figure 4: (a)&(b): Quad-dominant meshing of Lion model; (c):Quad-dominant meshing of a CAD model.

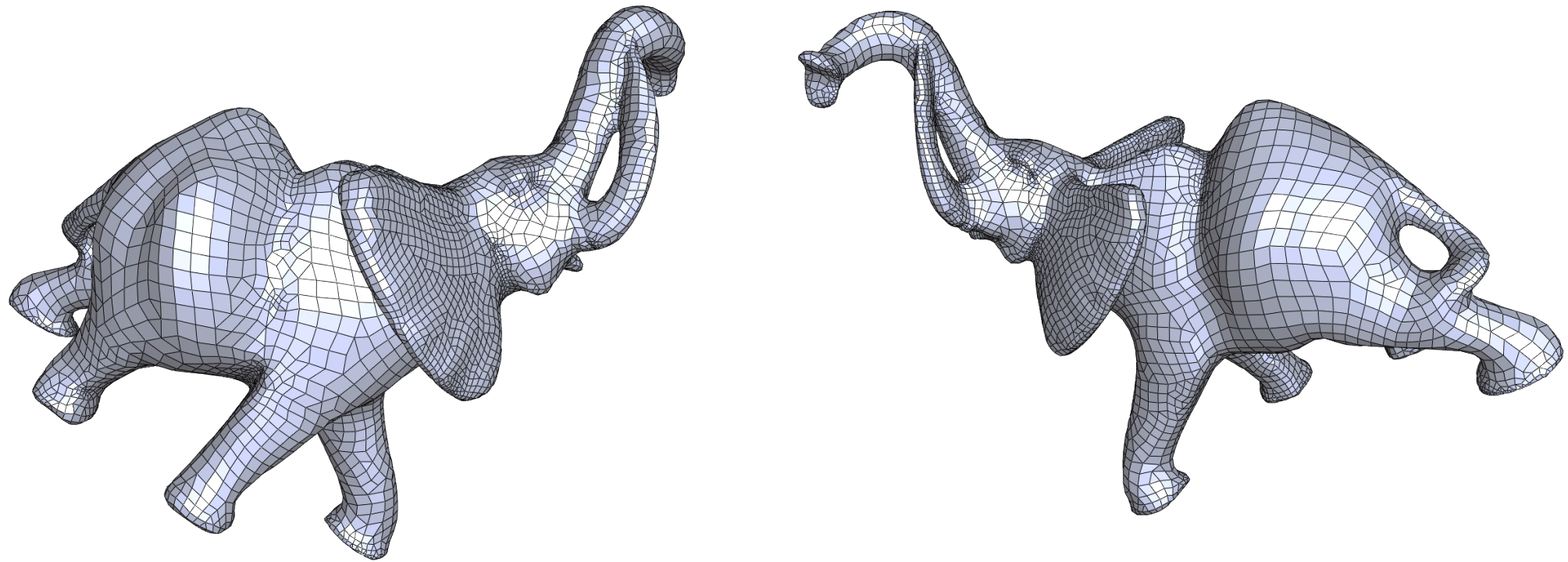


Figure 5: Adaptive Quad-dominant meshing. The density is set as the inverse of the squared local feature size.

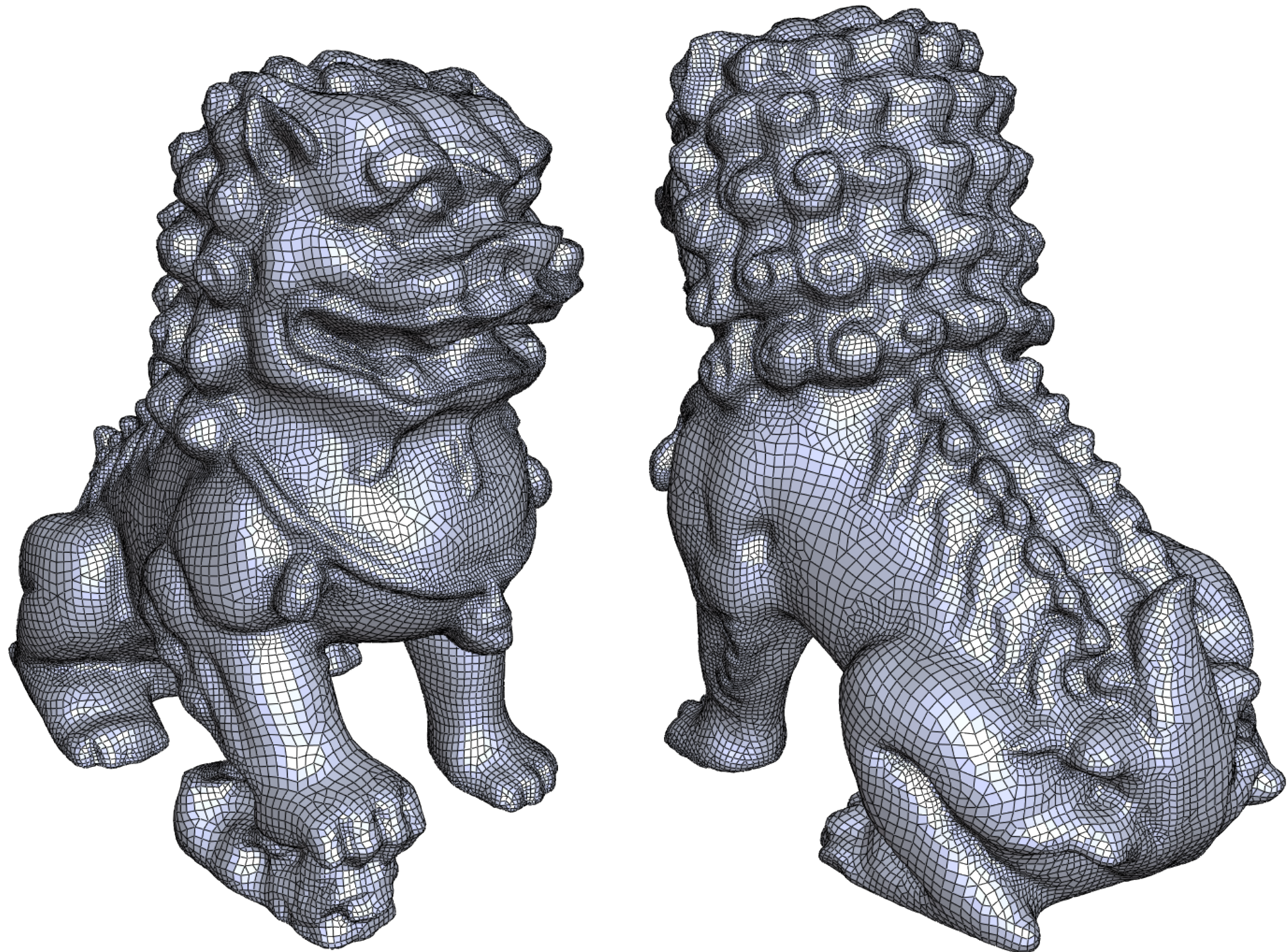


Figure 6: Adaptive Quad-dominant meshing. The density is set as the inverse of the squared local feature size.

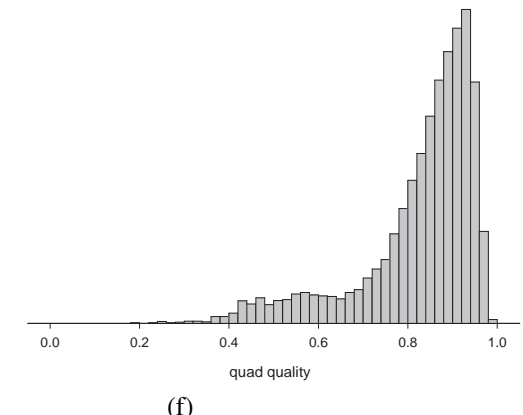
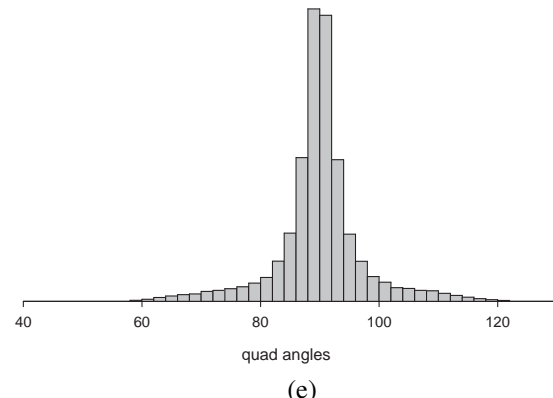
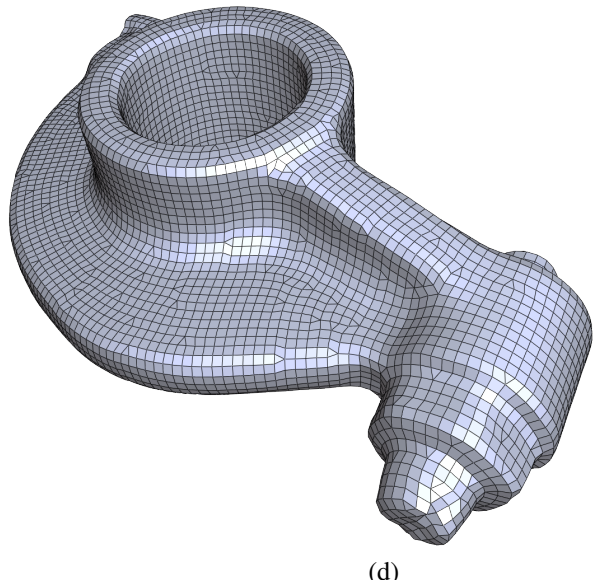
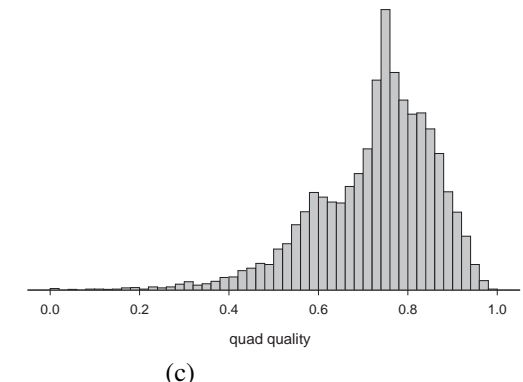
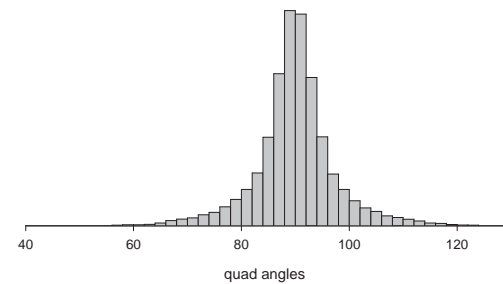
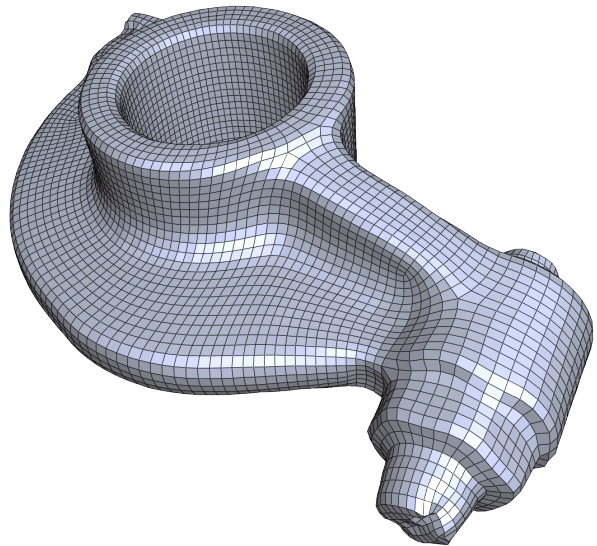
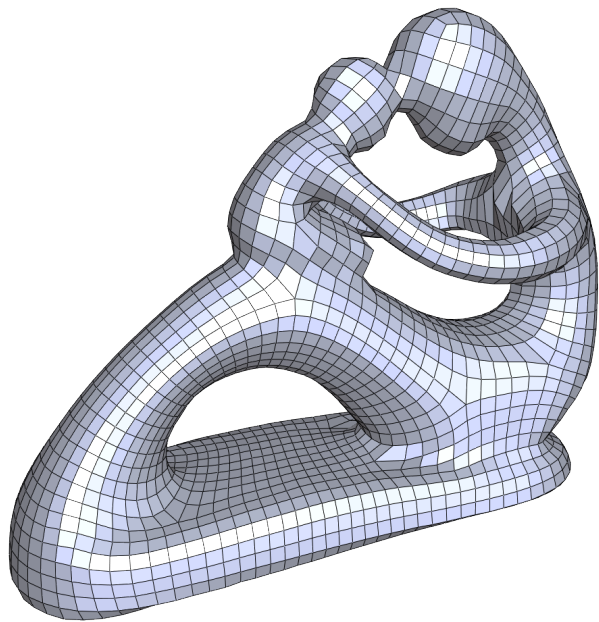
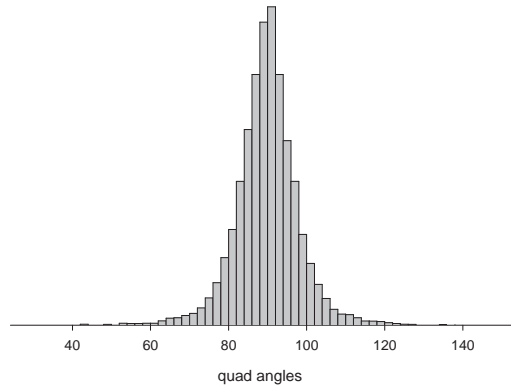


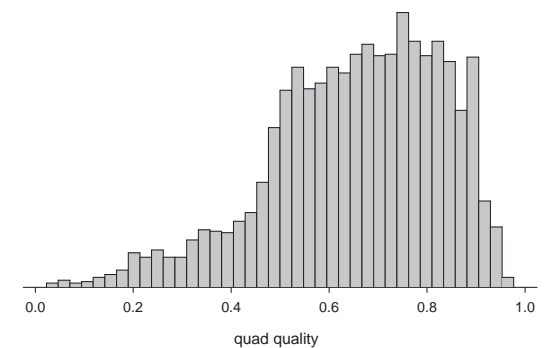
Figure 7: Comparison with [Mixed-Integer Quadrangulation, David Bommes et al. 2009]. Rockerarm Model (from www.graphics.rwth-aachen.de). (a-c): quadmesh by Mixed-Integer Quadrangulation, histogram of angles of quad faces and histogram of quality measure of quad faces; (d-e): our quad-dominant mesh and histograms. The definition of spacial quadrilateral quality is defined in [B. Joe, Shape measures for quadrilaterals, pyramids, wedges, and hexahedra, Technical Report, 2008] where the planarity is considered.



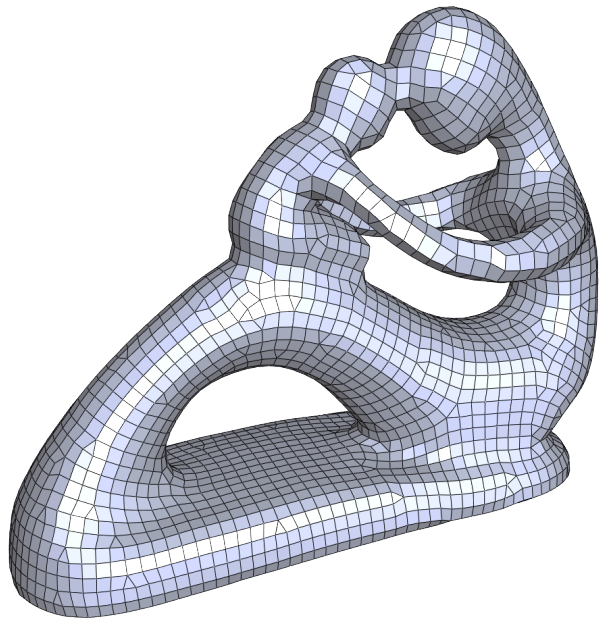
(a)



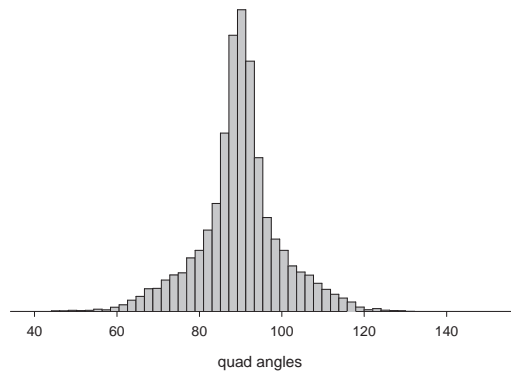
(b)



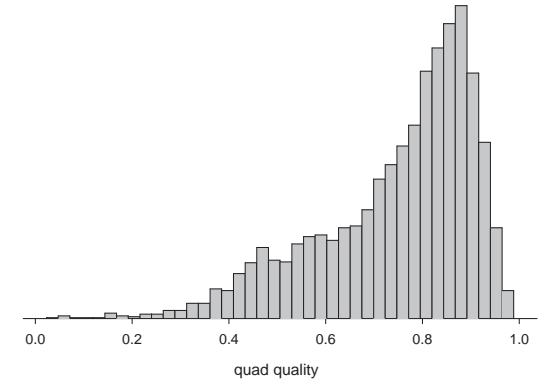
(c)



(d)



(e)



(f)

Figure 8: Comparison with Mixed-Integer Quadrangulation. Fertility Model (from www.graphics.rwth-aachen.de). (a-c): quadmesh by Mixed-Integer Quadrangulation, histogram of angles of quad faces and histogram of quality measure of quad faces; (d-e): our quad-dominant mesh and histograms.

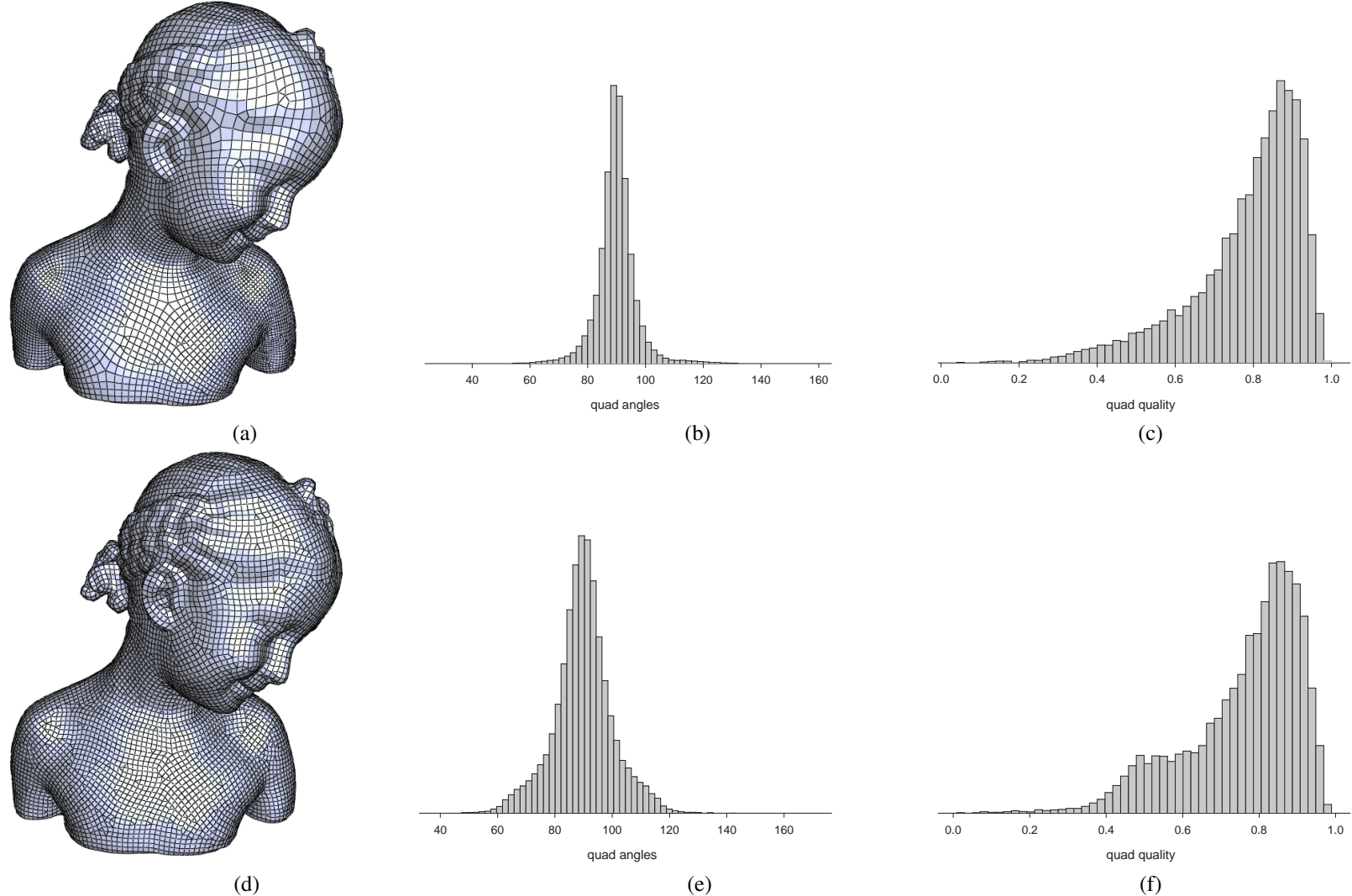


Figure 9: Comparison with Periodical Global Parameterization. Bimba Model (from AimShape). (a-c): quadmesh by Periodical Global Parameterization, histogram of angles of quad faces and histograms of quality measure of quad faces; (d-e): our quad-dominant mesh and histograms.

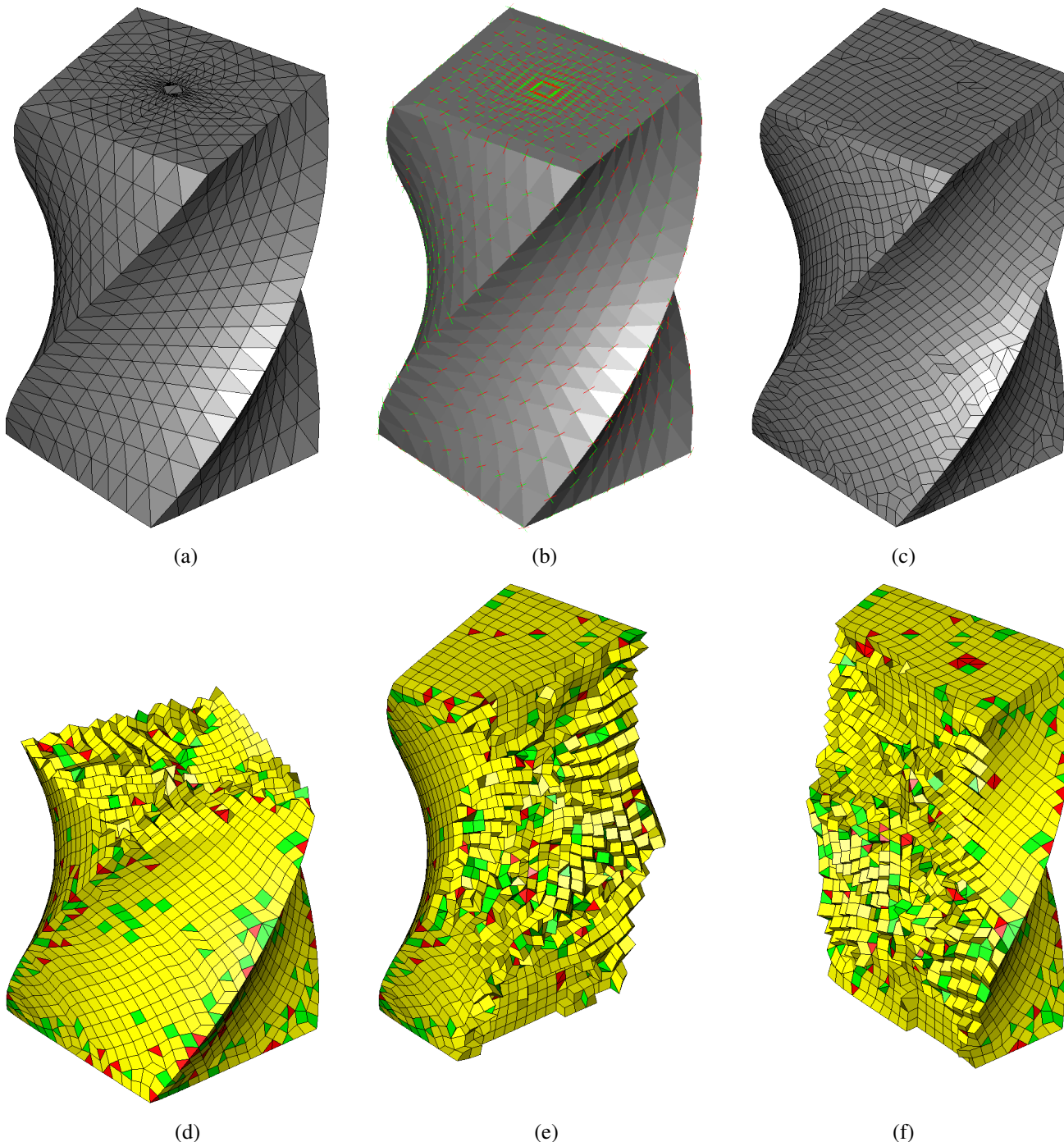
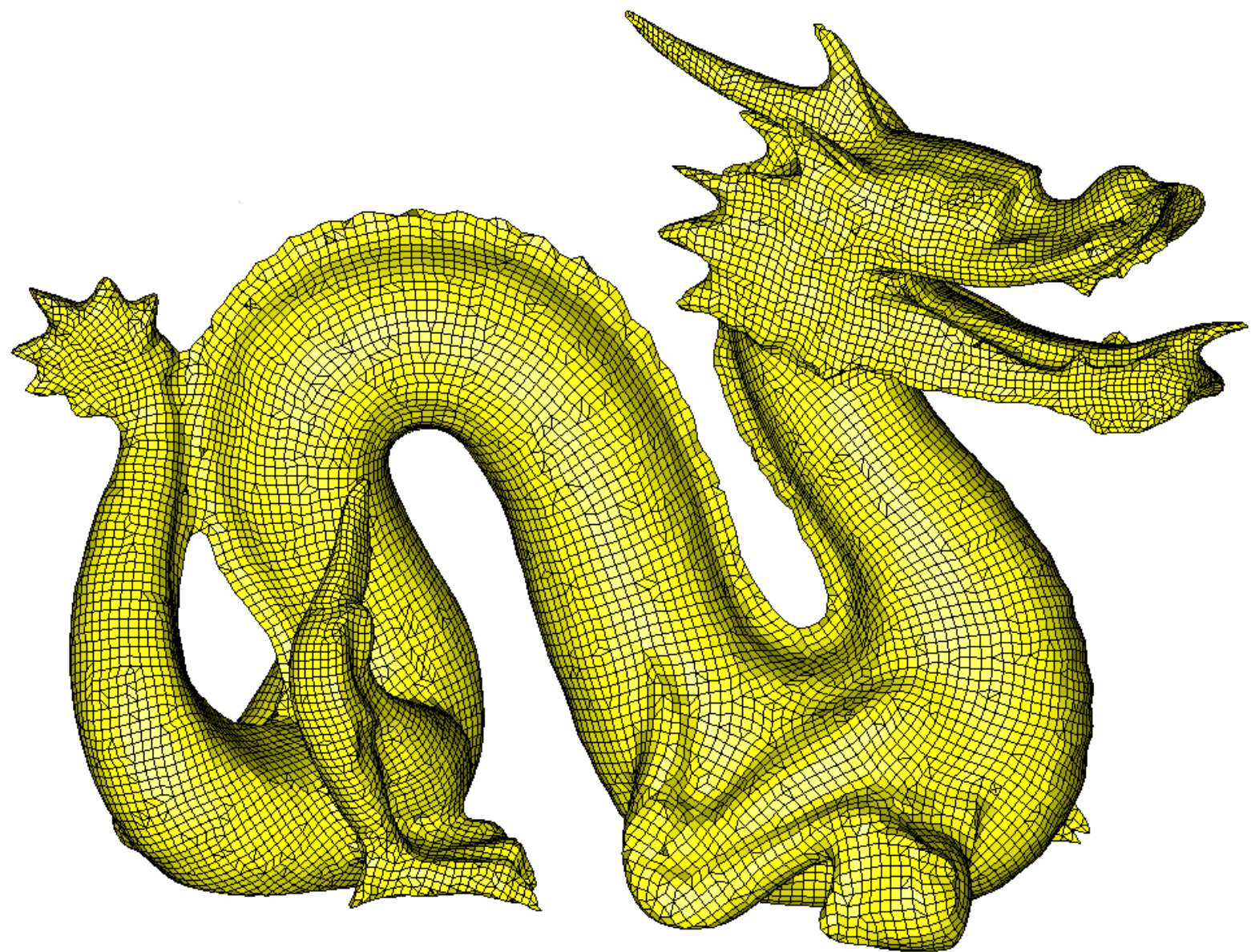
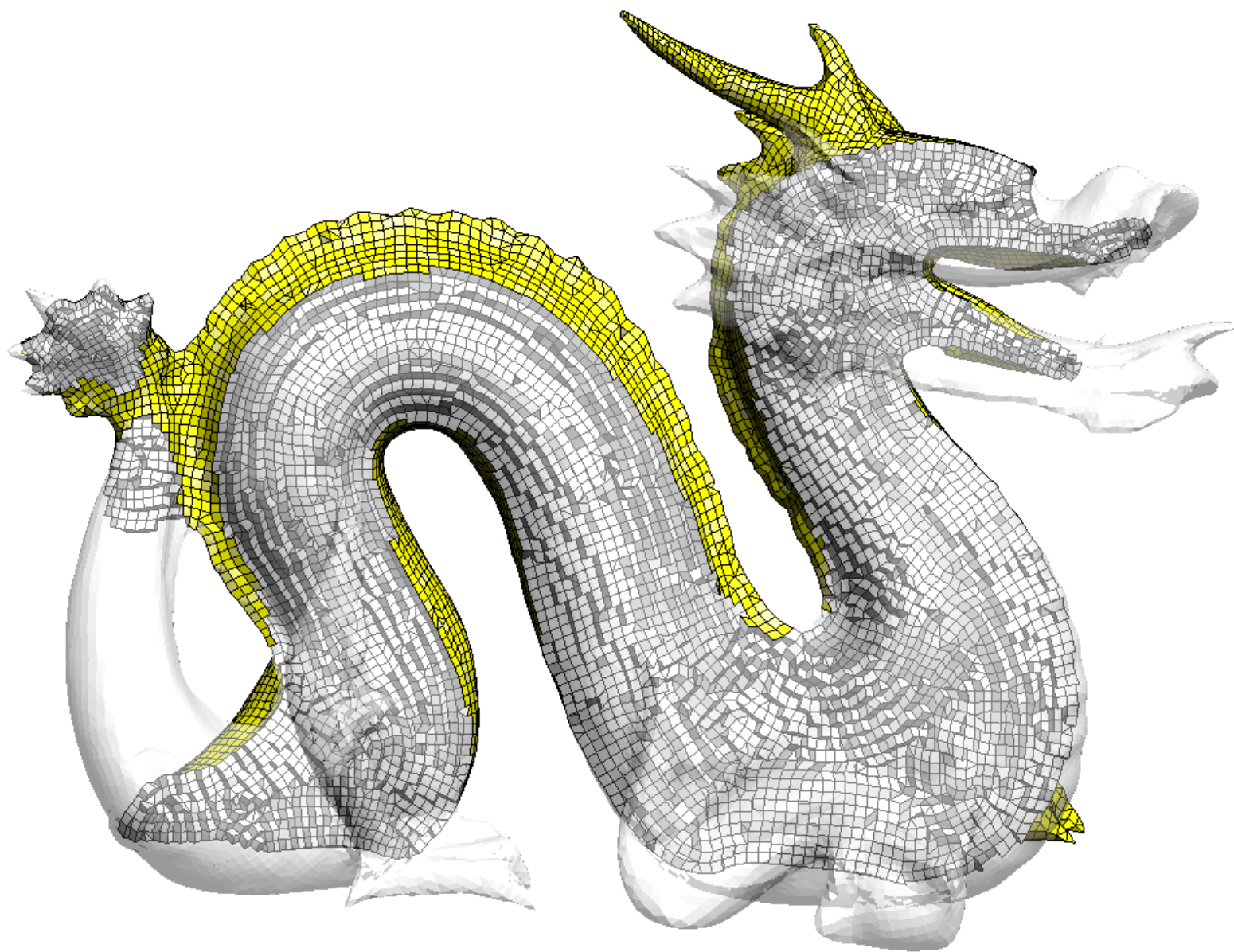


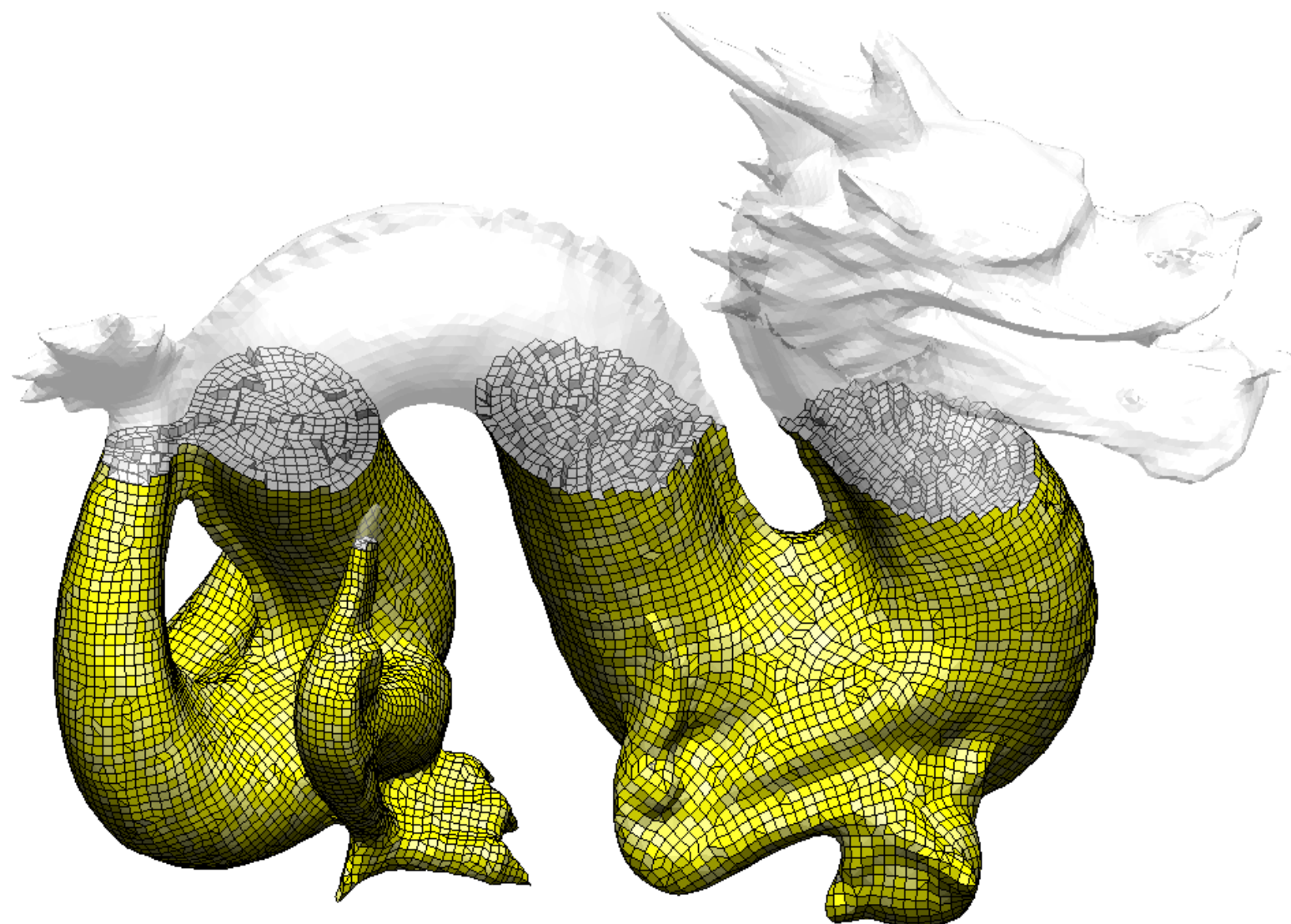
Figure 10: Hex-dominant meshing a pseudo cube. (a): the input model; (b): directional field; (c) the Hex-dominant meshing result; (d), (e) & (f): Clipping views of the Hex-dominant mesh (hexahedral elements in yellow, pyramidal elements in green and tetrahedral elements in red).



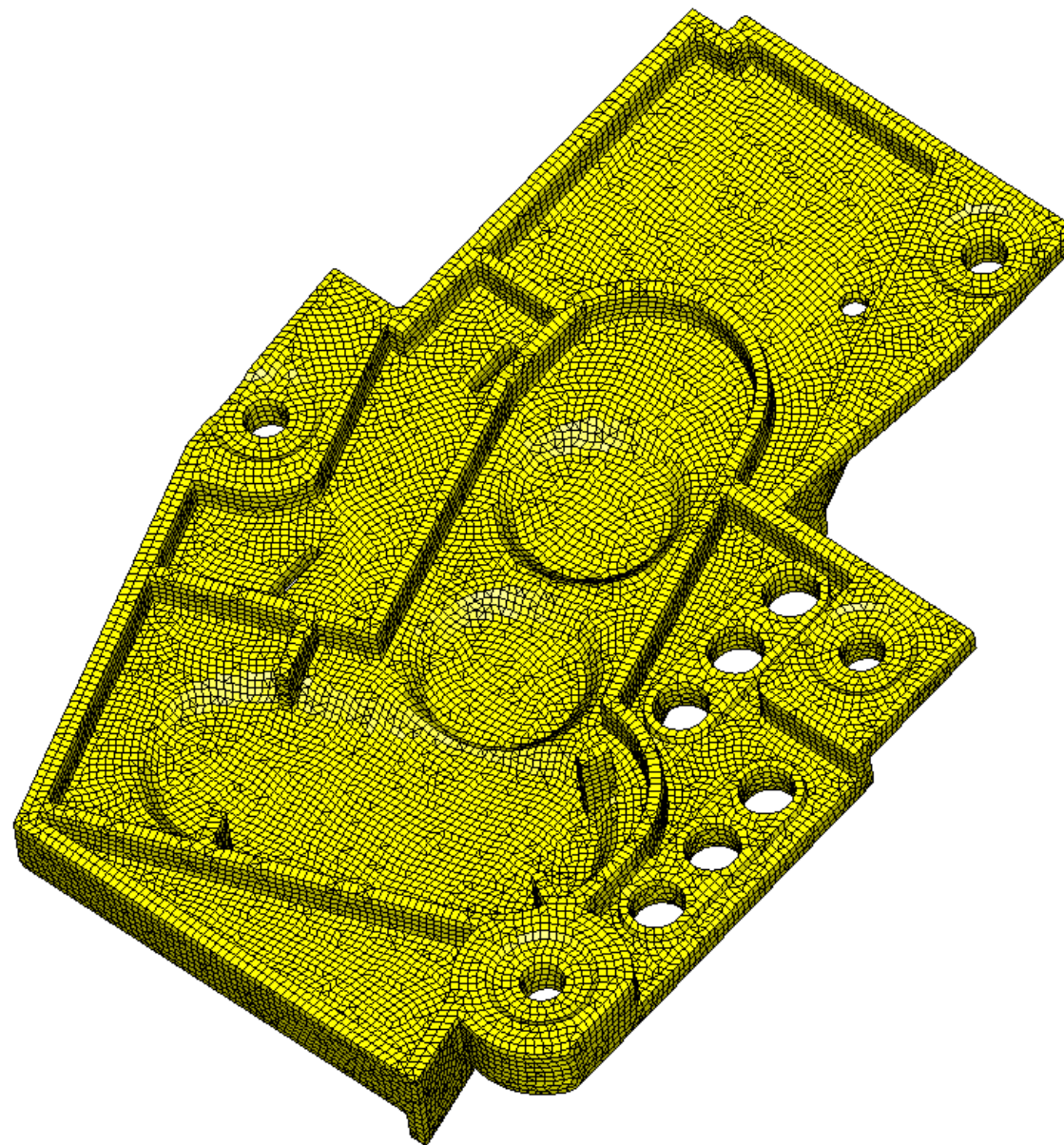
Hex-dominant meshing of the Dragon



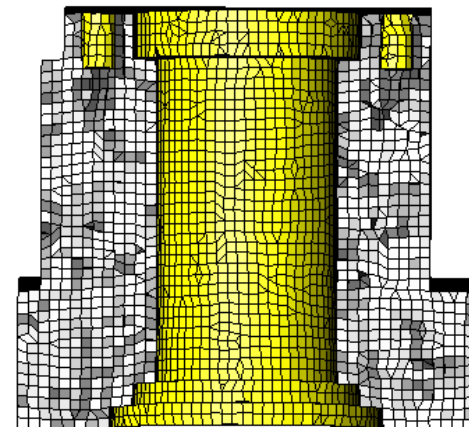
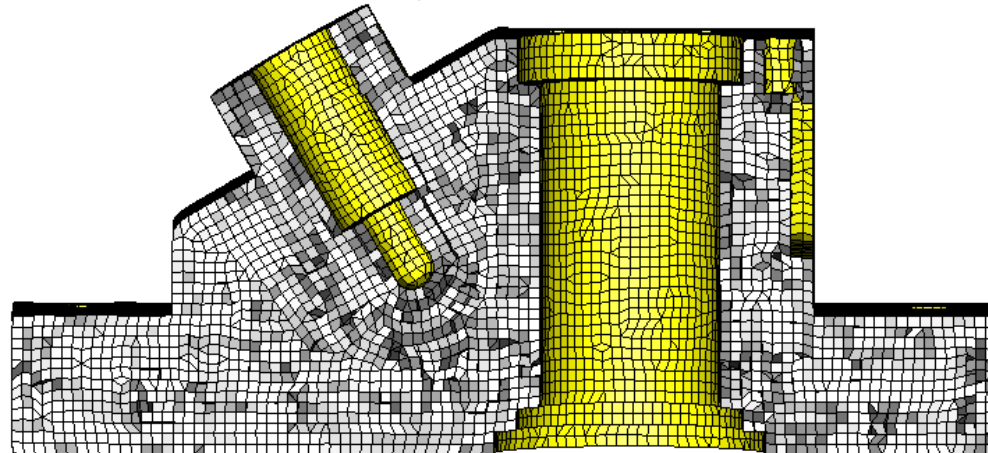
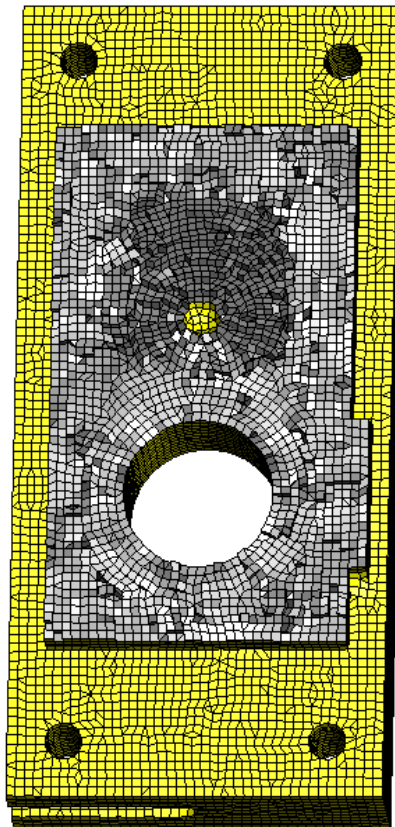
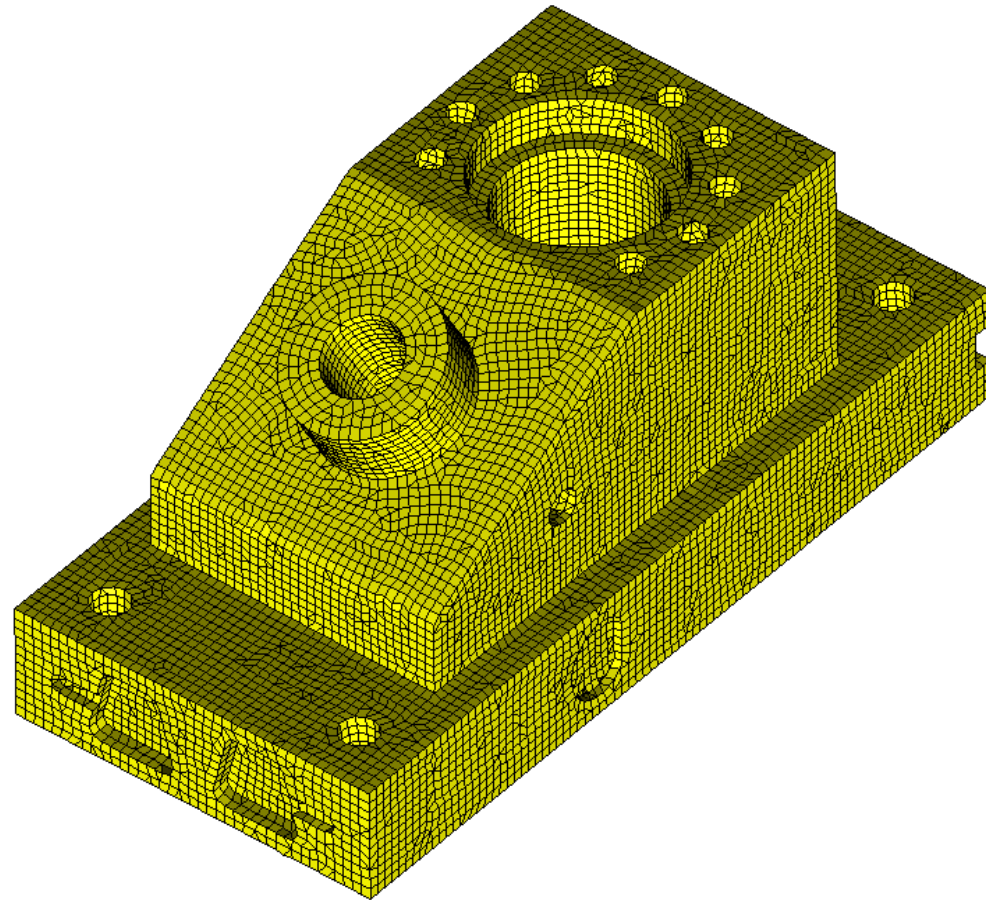
Hex-dominant meshing of the Dragon (cross-section).



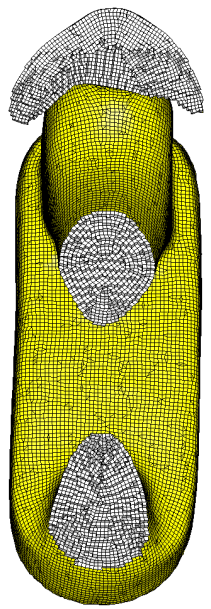
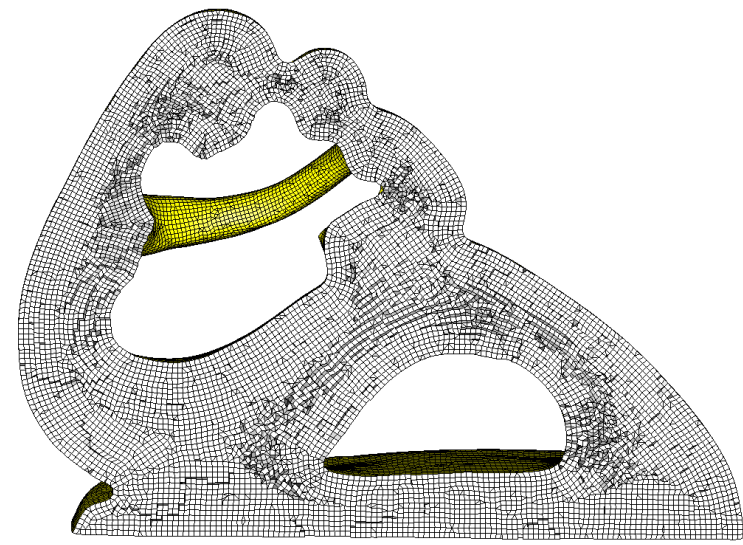
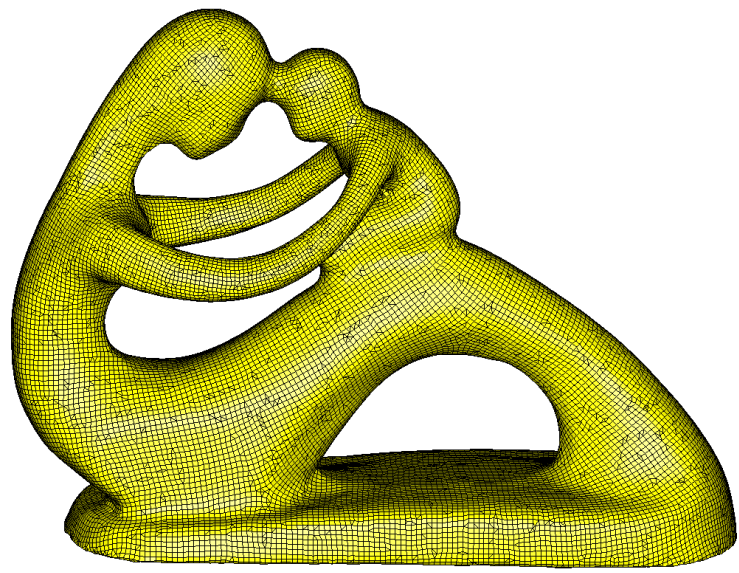
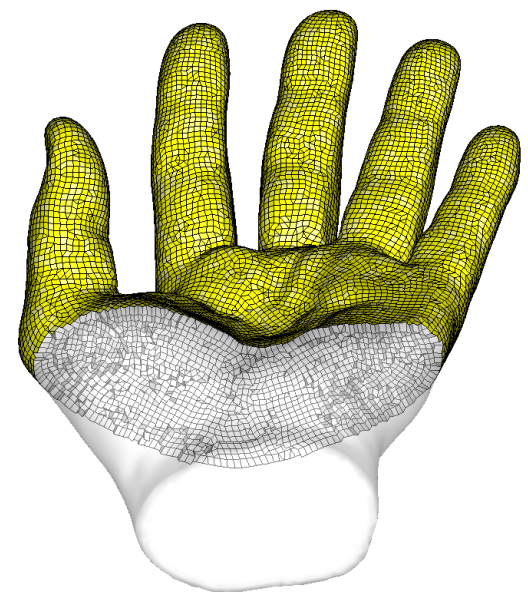
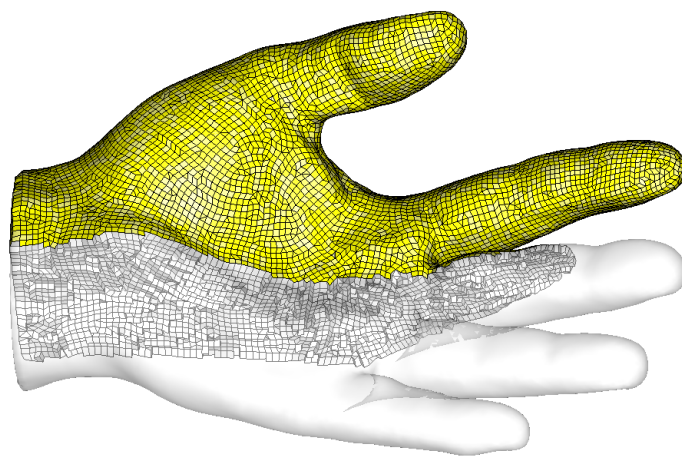
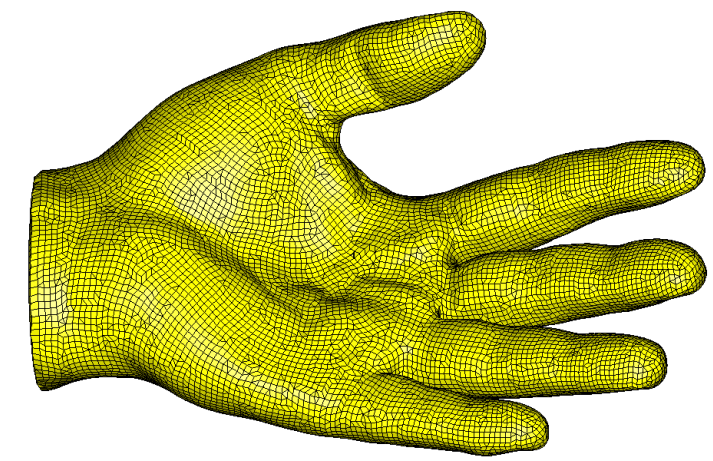
Hex-dominant meshing of the Dragon (cross-section).



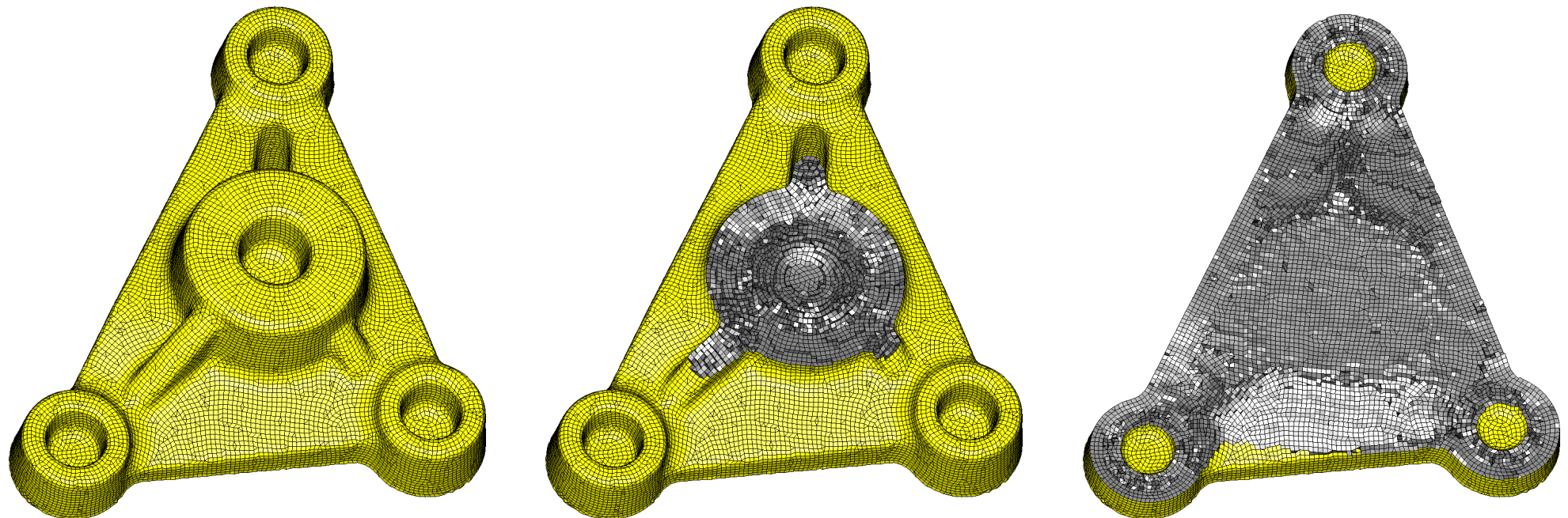
Hex-dominant meshing of a CAD model.



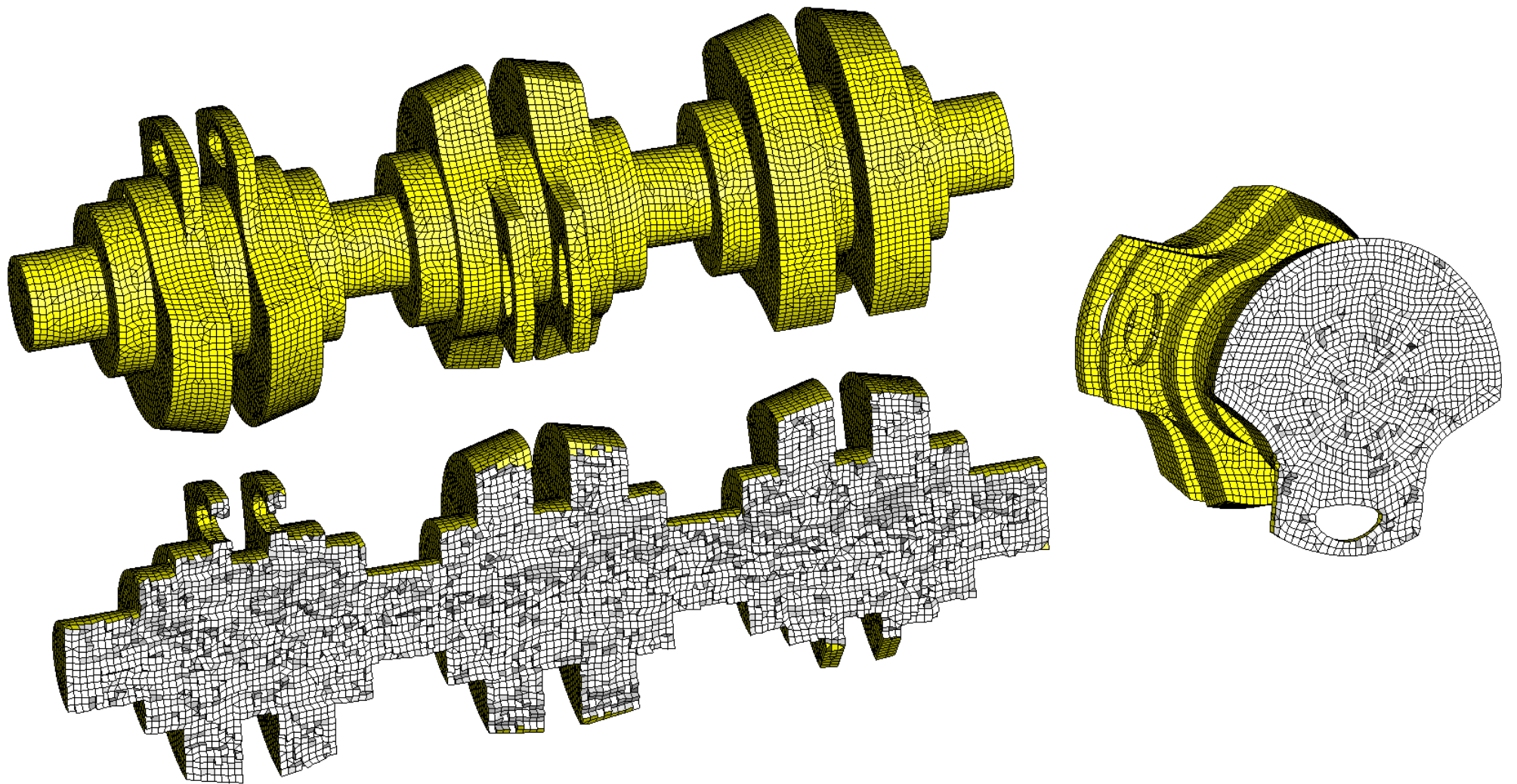
Hex-dominant meshing of a mechanical part and cross-sections.



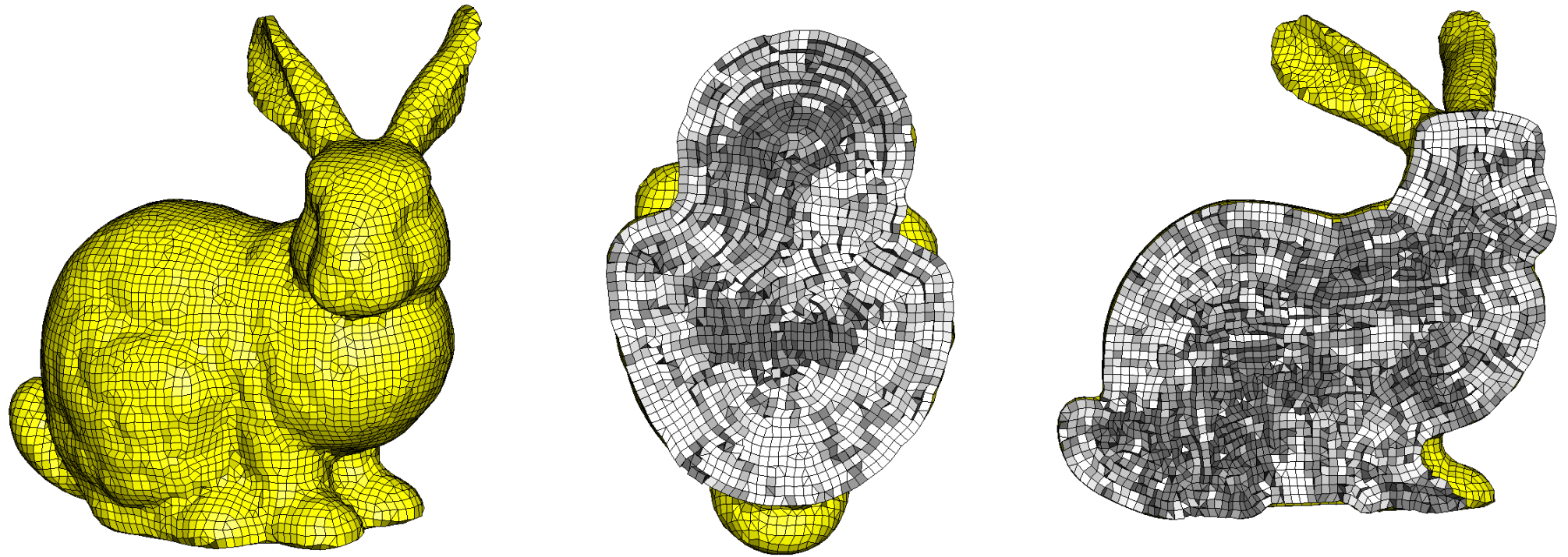
Hex-dominant meshes and cross-sections.



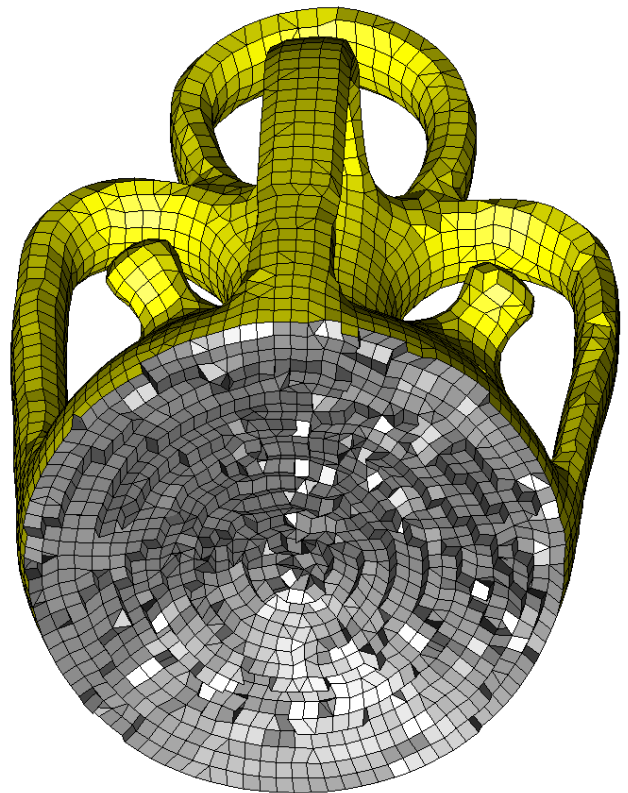
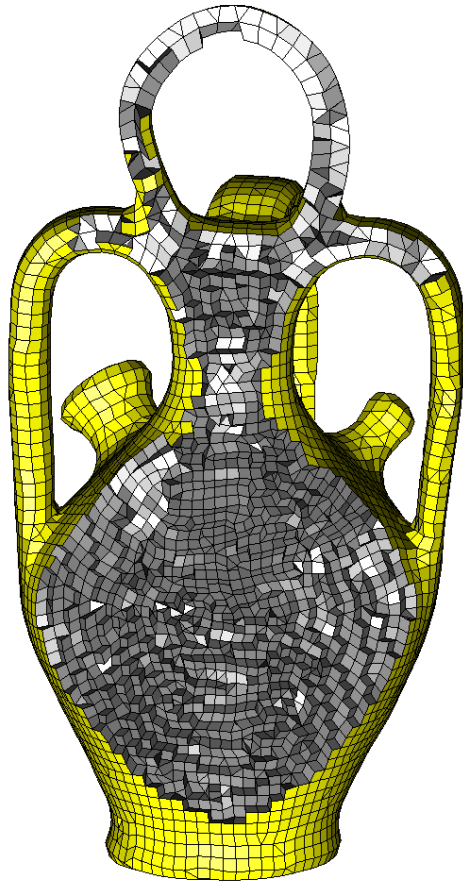
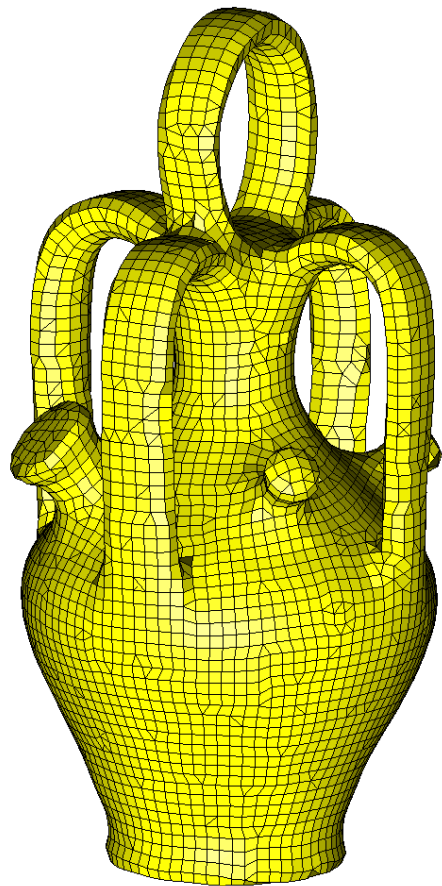
Hex-dominant meshing of a CAD model and cross-sections.



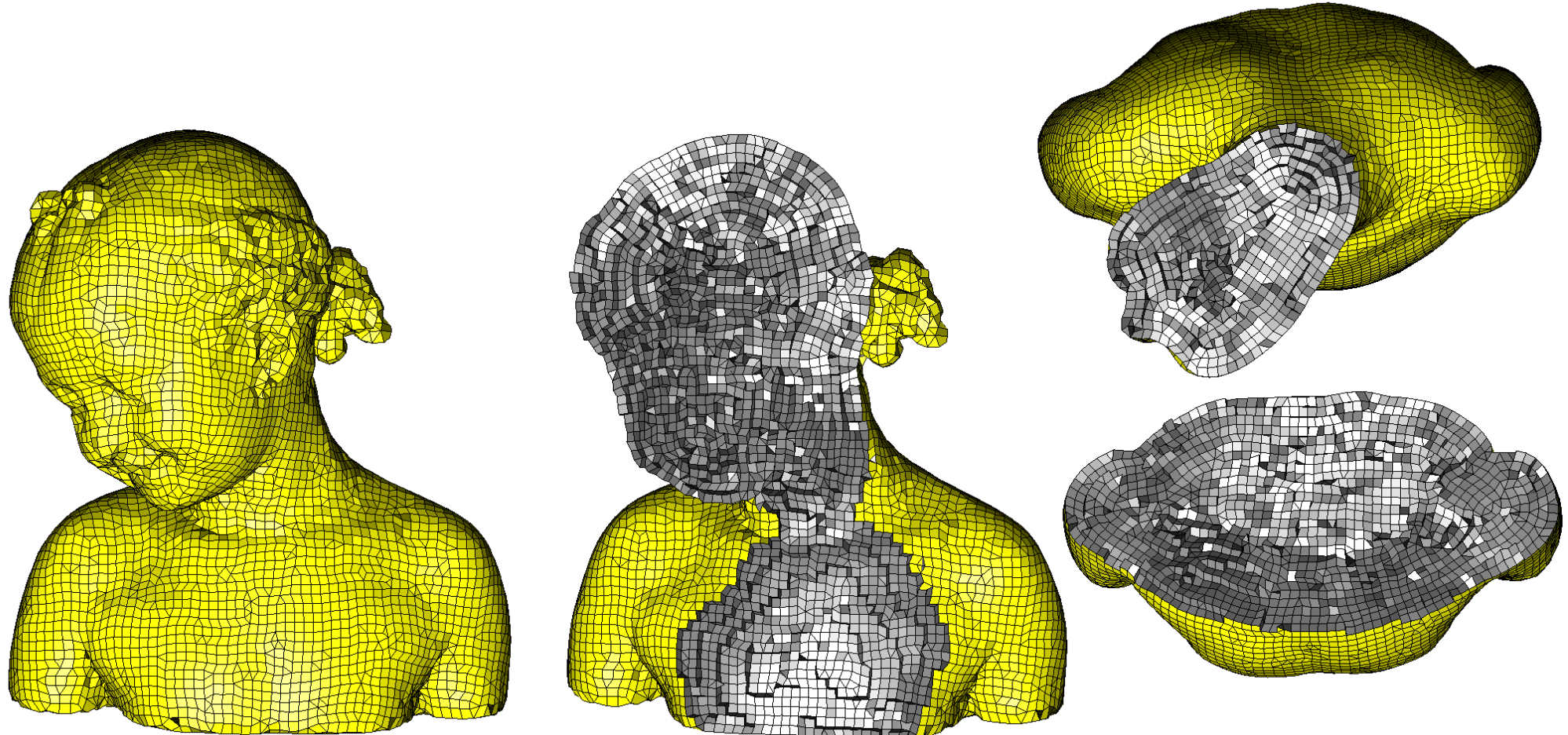
Hex-dominant meshing of a CAD model and cross-sections.



Hex-dominant meshing of the 'stanford Bunny' dataset



Hex-dominant meshing of the 'botijo' dataset



Hex-dominant meshing of the 'Bimba' dataset.